



City Research Online

City St George's, University of London

Citation: Sui, C., Wang, S., Liang, J. & Nomikos, N. (2025). Operating Capacity, Pricing and Supply Elasticity in Container Shipping Markets. *International Journal of Finance and Economics*, ijfe.70082. doi: 10.1002/ijfe.70082

This is the published version of the paper.

This version of the publication may differ from the final published version. To cite this item please consult the publisher's version.

Permanent repository link: <https://openaccess.city.ac.uk/id/eprint/36056/>

Link to published version: <https://doi.org/10.1002/ijfe.70082>

Copyright and Reuse: Copyright and Moral Rights remain with the author(s) and/or copyright holders. Copies of full items can be used for personal research or study, educational, or not-for-profit purposes without prior permission or charge, unless otherwise indicated, provided that the authors, title and full bibliographic details are credited, a hyperlink and/or URL is given for the original metadata page and the content is not changed in any way. For full details of reuse please refer to [City Research Online policy](#).

RESEARCH ARTICLE OPEN ACCESS

Operating Capacity, Pricing and Supply Elasticity in Container Shipping Markets

Cong Sui^{1,2} | Shang Wang¹ | Jingmin Liang² | Nikos K. Nomikos³

¹School of Maritime Economics and Management, Dalian Maritime University, Dalian, China | ²Collaborative Innovation Center for Transport Studies, Dalian Maritime University, Dalian, China | ³Bayes Business School, City St George's, University of London, London, UK

Correspondence: Nikos K. Nomikos (n.nomikos@city.ac.uk)

Received: 21 October 2024 | **Revised:** 30 July 2025 | **Accepted:** 9 October 2025

Funding: This work was supported by the National Natural Science Foundation of China (No. 72371045 and No. 71971034).

Keywords: capacity planning | container shipping markets | freight rates | international trade | marginal cost | operating capacity | supply elasticity

ABSTRACT

We investigate the channels through which changes in operating capacity influence freight rates in the container shipping market using a novel dataset to create an operating capacity index at the shipping-route level. Our analysis reveals that when supply elasticity is low, an increase in operating capacity tends to drive freight rates upward, as the market faces constraints and cannot easily accommodate additional demand. Conversely, when supply elasticity is high, an increase in operating capacity generally leads to lower freight rates since additional capacity can be deployed to meet rising demand, preventing price surges. These findings suggest that shipping companies strategically adjust capacity based on market conditions to optimise profitability, shifting between price and quantity competition depending on route characteristics and supply elasticity.

JEL Classification: D40, L91

1 | Introduction

Containerisation has revolutionised global trade, significantly reducing transport times and costs (Hummels 2007). This has been a key driver of the growth in global trade in recent decades (Bernhofen et al. 2016; Coşar and Demir 2018). The contribution of container trade to global economic activity is well documented (Kilian et al. 2023). Today, 60% of the value of seaborne trade and nearly 90% of non-bulk dry cargo is transported as containerised cargo, including most manufactured and high-value-added goods. For instance, European and US manufacturing firms rely on imports of containerised raw materials and intermediate goods, while consumers routinely purchase finished goods delivered in containers.

The cost of seaborne transportation, particularly freight rates, directly impacts economic growth. Various factors influence

these rates, including supply and demand uncertainty, fleet utilisation, competitor behaviour and geopolitical considerations (Kilian et al. 2023; Michail and Melas 2021; Li et al. 2023).¹ Lower transportation costs and times lead to rapid growth in world trade and economic development (Pascali 2017). Similarly, as shipping freight rates are among the most volatile asset classes (Choi et al. 2020; Pouliasis and Bentsos 2024), understanding the determinants of containership freight rates is crucial for both shipping and commodity markets.

Previous research has primarily focused on the impact of changes in supply and demand factors on freight rates. From a supply perspective, the emphasis has been on how changes in the operational fleet size affect freight rates. However, this static measure of supply overlooks an important dimension: the intensity of container fleet utilisation over time. This is often due to the lack of accurate measures of fleet utilisation at high frequency.

This is an open access article under the terms of the [Creative Commons Attribution](https://creativecommons.org/licenses/by/4.0/) License, which permits use, distribution and reproduction in any medium, provided the original work is properly cited.

© 2025 The Author(s). *International Journal of Finance & Economics* published by John Wiley & Sons Ltd.

In this paper, we address this shortcoming of previous research by estimating the level of utilisation using highly granular data that measures the number of container ships operating on each shipping route in real time. Specifically, we construct operating capacity indices at the shipping-route level using a novel dataset that monitors vessel deployment across different container shipping routes. These indices are based on Automatic Identification System (AIS) data on containership movements and port calls, providing detailed micro-information on how container operating capacity varies over time and across trade routes.² This enables us to examine how operating capacity affects freight rates and how companies deploy their ships in response to competition and changing market dynamics.

Our paper contributes to the literature in several ways. First, it provides empirical insights into the organisation and structure of container shipping markets. It discusses how shipping companies deploy their assets and respond to changing market dynamics by switching between price and quantity competition. This aligns with the work of Tvedt and Hovi (2024). Second, the paper uses a novel dataset to construct operating capacity indices for individual shipping routes. This extends the studies of Regli and Nomikos (2019) and Li et al. (2022), which analysed micro-dynamic market information from shipping big data. It also adds to the expanding literature on the provision of novel datasets for the container sector, as highlighted by Otani and Matsuda (2023). Recent studies, such as Li et al. (2024) and Zheng et al. (2024), also examine how changes in operating capacity affect freight rates and freight volatility, respectively. However, these studies differ from ours in that they use monthly and quarterly data, respectively, and do not distinguish between periods of high and low idle capacity. This distinction is crucial, as the response of freight rates to changes in capacity depends on the shape and elasticity of the supply curve.

Finally, the paper provides empirical support for the theoretical predictions of earlier studies, such as Koopmans (1939), Wergeland (1981) and Stopford (2009), on the shape of the shipping supply curve and confirms recent empirical evidence that capacity constraints generate convex supply curves (Boehm and Pandalai-Nayar 2022). Thus, the paper complements empirical research on dynamic pricing conditional on idle capacity (Elmaghraby and Keskinocak 2003) and asset pricing for shipping markets (Drakos and Tsouknidis 2024).

We find that the response of freight rates to changes in operating capacity is conditional on the level of idle capacity in the market. When idle capacity is high, changes in operating capacity are significantly negatively correlated with freight rates. This is consistent with shipping companies reducing their capacity in periods of low utilisation to increase their revenue, as the increase in freight rates outpaces the reduction in capacity due to the inelastic demand for shipping services. On the other hand, when fleet utilisation is high, shipping companies respond to increases in transportation demand by increasing vessel speed, which results in higher fuel consumption and voyage costs. They also rotate less efficient vessels from other shipping routes, which increases operating costs. Both measures increase the marginal cost of containerised shipping and result in higher transportation costs per unit of cargo.

The rest of the paper is structured as follows: Section 2 discusses the characteristics of the container shipping market and analyses it using the theories of supply elasticity and marginal cost. Section 3 describes the construction of the operating capacity index and presents its statistical properties. Section 4 analyses the predictive power of operating capacity on freight rates. Section 5 checks the robustness of the empirical results. Finally, Section 6 concludes the paper.

2 | Institutional Background of Container Shipping Markets

The intermodal transportation of cargo in reusable containers of standardised dimensions has revolutionised global trade since the 1960s and has played a central role in the globalisation of the economy since the 1990s, mainly due to its advantages of cost-effectiveness, flexibility and integrability.

Container shipping markets are an integral part of the modern, highly interconnected global supply chains. The latter are a major source of productivity gains but, at the same time, the tight network of global sourcing makes countries vulnerable to disruptions as manifested during the COVID-19 pandemic. The quantifiable impact of disruptions in container shipping markets is well documented. Finck and Tillmann (2022) find that global supply chain shocks account for up to 30% of inflation dynamics and have an impact both on real economic activity and on consumer prices in the Eurozone area. Similarly, the reduction of frictions in containership trades, in the form of easing bottlenecks and port congestion, led to a faster recovery of US manufacturing and increased the post-pandemic recovery of real demand in the US by up to 18% (Kilian et al. 2023). It also seems that the impact of supply chain disruptions differs according to their origin. For instance, Finck and Tillmann (2022) find that supply chain disruptions originating in China are an important driver for changes in industrial production, while disruptions originating outside of China are an important driver for the dynamics of consumer prices.

The primary aims of container shipping companies are to increase their market share and avoid having idle capacity by deploying it to the market (Song and Wang 2022). This enables them to exploit economies of scale (Cullinane and Khanna 2000) but also leads to fierce competition, low profit margins and chronic oversupply. To survive such a competitive environment, major global carriers form alliances that involve co-deployment of ships over certain routes to improve capacity utilisation, reduce operational costs and ultimately achieve economies of scale.

Nowadays, shipping alliances have become a prevalent form of cooperation among major container shipping companies. By forming an alliance, shipping companies can exchange their container slots to better adapt to the uncertain shipping demand and improve capacity utilisation. Both excess ship capacity and shipping demand affect the optimal slot allocation and exchange strategy in the alliance. Larger shipping capacity leads to more excess slots exchanged within the alliance to transport more containers but with an overall reduction in capacity utilisation. A stronger shipping demand leads to more containers being transported by competitors due to limitations of shipping

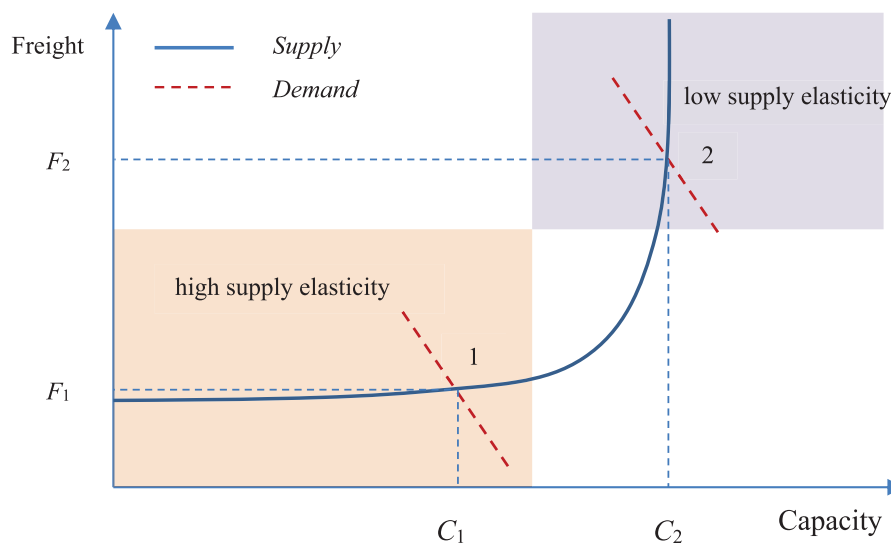


FIGURE 1 | Supply elasticity of the shipping market. [Colour figure can be viewed at [wileyonlinelibrary.com](https://onlinelibrary.wiley.com/doi/10.1002/ijfe.70082)]

capacity and higher capacity utilisation. Quite often, faced with higher demand uncertainty, shipping companies choose to keep excess spare capacity, which results in lower profit margins.

From an economic point of view, the shipping freight rate is the equilibrium price in the shipping market, reflecting the balance between supply and demand for a specific trading route. The freight rate is therefore the projection of the intersection of the supply curve and the demand curve on the price axis. On the other hand, the operating capacity index that we develop in the paper measures the actual level of capacity for each specific route and can thus be viewed as the projection of the intersection of the supply and demand curves on the quantity axis.

In shipping markets, the relationship between operating capacity and freight rates depends on supply elasticity and marginal cost. The price elasticity of supply is the degree to which supply responds to price changes. The supply schedule for shipping markets is unique and differs from that of other commodity markets in that it can shift from *horizontal* to *vertical* over a range of freight rates, as shown in Figure 1 (Stopford 2009). Previous studies suggest that idle capacity is related to the elasticity of supply (Koopmans 1939; Wergeland 1981). Supply is elastic when there is excess idle capacity in the market (Area 1 in Figure 1). In this case, a short-term increase in demand will not have a noticeable impact on freight rates. On the other hand, supply is inelastic when the fleet is fully utilised and there is no spare capacity in the market (Area 2 in Figure 1); in this case, a shift in demand will lead to significant freight rate fluctuations (Alizadeh and Nomikos 2007; Nomikos and Tsouknidis 2022).

Marginal cost refers to the increase in total cost for each additional unit of product (or service). Containerships typically carry from a few thousand to tens of thousands of twenty-foot equivalent units (TEUs). As the utilisation rate of the fleet increases, the marginal cost of transportation increases as well. In addition, freight rates often differ by the direction of transportation and there is a large directional imbalance between freight rates for fronthaul voyages (i.e., voyages in the main direction of trade that involve larger cargo volumes) and backhaul freight

rates (i.e., the return leg where cargo volumes are generally lower and containerships mostly transport empty container boxes) (see e.g., Brancaccio et al. 2020). Container boxes are valuable assets in their own right and their timely positioning is important for the smooth functioning of global supply chains. Often, in periods of strong demand, container companies prefer to ship containers back to their ports of origin empty in order to fill them up as soon as possible (Kilian et al. 2023). The transportation of empty containers leads to higher transportation costs, which may be as high as 20% of the total operating costs. As a result, when cargo volumes are low and sufficient idle capacity exists in the market, an increase in carrying capacity for a specific route can significantly reduce the cost of transporting individual containers.

3 | Construction of the Operating Capacity Index

We construct the container operating capacity index by combining AIS data on containership port calls with information about the physical characteristics of ships, obtained from the International Maritime Organisation (IMO). Our focus is on trade routes that originate from China, which is the world's leader in maritime connectivity and total cargo movements (Saeed and Cullinane 2023). In 2022, China's container port throughput was 300 million TEUs, accounting for about 35% of the global container port throughput,³ and China's Liner Shipping Connectivity Index (LSCI)⁴ was ranked first in the world, making it the most connected economy in the global container shipping network.

We focus on nine container shipping routes originating from China, namely the Japan route, Europe route, U.S. West Coast route, U.S. East Coast route, South Korea route, Southeast Asia route, Australia/New Zealand route, South Africa route and South America route. According to the 2023 data from the General Administration of Customs of the People's Republic of China, the countries and regions covered by those nine routes account for 77.02% of total Chinese containerised trade. Table 1 shows the nine shipping routes, including the variable names

TABLE 1 | Containerised freight indices and routes.

Shipping routes	Operating capacity indices	CCFI	Ports/countries
Japan route	Cap ¹ / Num ¹	Fre ¹	Japan (all ports)
Europe route	Cap ² / Num ²	Fre ²	Hamburg, Rotterdam, Antwerp, Felixstowe and Le Havre
U.S. West Coast route	Cap ³ / Num ³	Fre ³	Los Angeles, Long Beach, Seattle, Oakland and Tacoma
U.S. East Coast route	Cap ⁴ / Num ⁴	Fre ⁴	New York-New Jersey, Savannah and Houston
S. Korea route	Cap ⁵ / Num ⁵	Fre ⁵	Korea (all ports)
Southeast Asia route	Cap ⁶ / Num ⁶	Fre ⁶	Singapore, Vietnam, Malaysia and Thailand
Australia/New Zealand route	Cap ⁷ / Num ⁷	Fre ⁷	Australia and New Zealand
South Africa route	Cap ⁸ / Num ⁸	Fre ⁸	South Africa (all ports)
South America route	Cap ⁹ / Num ⁹	Fre ⁹	Brazil, Colombia, Peru, Chile and Ecuador

Note: The first column shows the names of the nine routes; the second and third columns show the variable names of the operating capacity indices and the China Containerised Freight Index (CCFI), respectively. Finally, the fourth column shows the ports or countries covered by each route.

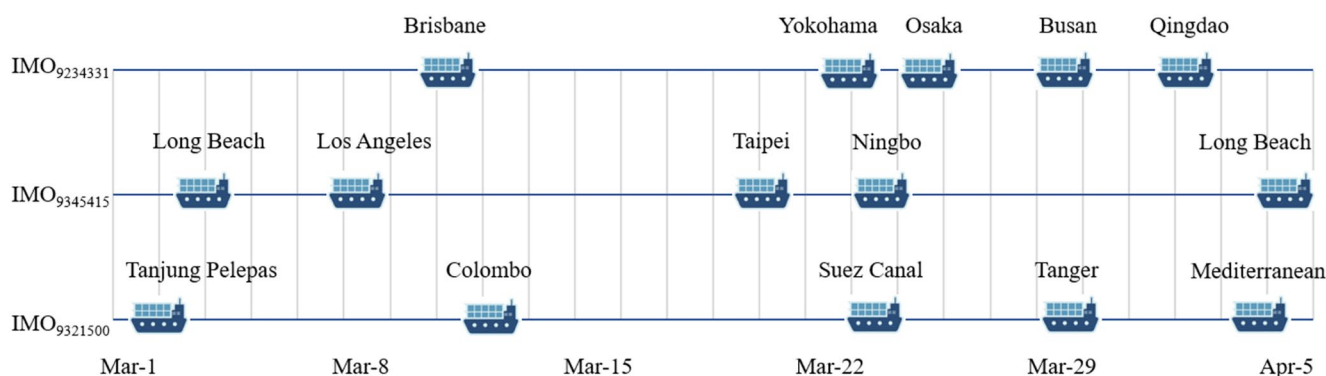


FIGURE 2 | Schematic diagram of vessels' port calls and docking track for three randomly selected vessels. [Colour figure can be viewed at [wileyonlinelibrary.com](https://onlinelibrary.wiley.com)]

and the ports/countries based on which the operating capacity index is constructed.

To construct the operating capacity index, we collect AIS data on containership port calls and dockings, which provide detailed information on the movements of each ship. AIS data have temporal and spatial attributes and include both dynamic and static information. The dynamic data contain time-stamped information, in Universal Standard Time (UST), on vessels' position (latitude and longitude), heading and speed, which is usually updated every 6s. The static information contains the IMO number, a unique identification number for each ship and information on the type of vessel. Figure 2 shows the docking track for three randomly selected containerships. For example, the container vessel with IMO number 9345415 departed from Long Beach to Los Angeles on 3 March 2022, and then departed from Los Angeles to Taipei on 8 March 2022.

Docking track data is then matched, via the IMO number, with data on vessels' particulars. The combined dataset includes static data such as the IMO number, gross tonnage and capacity of containerships, measured in TEUs and the docking track data

such as the port name, country or region and arrival/departure time of the departure/arrival port.

The operating capacity index for each shipping route is then constructed using the following steps:

Step 1: Determine the Origin and Destination of the Shipping Routes The starting point is to determine the origin and destination of the different shipping routes. For shipping routes to Europe, US West Coast and US East Coast, we identify the largest ports, in terms of container throughput, that belong to the respective regions. For example, destination ports on the US West Coast route include the ports of Los Angeles, Long Beach, Seattle, Oakland and Tacoma. For the remaining routes, we choose ports in the respective destination countries or areas. The ports and countries for each route are shown in Table 1.

Step 2: Remove Outliers For each containership voyage, we mark the points of origin and destination to determine the shipping route to which it belongs. This identification process results in inconsistencies in the data, which are mainly due to three factors: transit routes, outliers in voyage duration and

outliers in voyage trajectories. (1) Transit routes: The identification methodology does not distinguish between vessels doing shorthaul routes or additional port calls on their way to the final destination. For example, a voyage where a vessel departs from Qingdao and calls at the port of Busan (S. Korea) on her way to the US West Coast may be categorised as belonging to the Korea route, while the port of Busan is merely a transit port for the U.S. West route. Given that the vessels operating on the Korea, Japan and Southeast Asia routes are smaller, we impose an additional restriction that only small containerhips—with a capacity of less than 3000 TEUs—are considered when identifying voyages on the Korea and Japan routes; similarly, the criterion for determining voyages for the Southeast Asia route is a capacity of less than 8000 TEUs. (2) Outliers in voyage duration: Due to inconsistencies in AIS data, there are cases where the sailing time from origin to destination, point O to point D, is exceptionally long or short. To filter these outliers, we set lower and upper limit thresholds for the sailing time for each route, equal to the 5th and 95th percentiles, respectively. Sailing times outside of these two thresholds are excluded. (3) Outliers in voyage trajectories: There are generally many feasible trajectories from point O to point D on a given shipping route. Among the trajectories, some occur very infrequently. In the paper, voyages with trajectories that occur less than 10% of the time are removed.

Step 3: Calculate the Operating Capacity for Each Shipping Routes

We construct weekly operating capacity indices using the number of containerhips operating on a shipping route over the previous 7 days and their respective capacities, measured in TEUs, denoted as Num and Cap, respectively. For each of those metrics we consider three variants: Cap_A and Num_A measure, respectively, the fronthaul capacity and number of containerhips in the direction from the port of origin O to the destination port D; Cap_B , Num_B measure the backhaul capacity and number of containerhips in the reverse direction from the destination port D to the port of origin O; and Cap_C and Num_C measure the total capacity and number of containerhips and are calculated as the sum of the corresponding A and B indices. We use weekly time series data to construct the operating capacity indices for the period from January 2014 to May 2023. Detailed descriptions of the six operating capacity indices are shown in Table 2.

We also collect data on Idle capacity, $Idle_t$, defined as the combined TEUs of containerhips that are idle.⁵ Idle capacity is a reliable proxy for modelling supply elasticity (Boehm and Pandalai-Nayar 2022). We introduce two thresholds, δ_{high} and δ_{low} , to create two dummy variables that measure high and low operating capacity.

$$Id_t^H = \begin{cases} 1 & \text{when } Idle_t \geq \delta_{high} \\ 0 & \text{when } Idle_t < \delta_{high} \end{cases}$$

$$Id_t^L = \begin{cases} 1 & \text{when } Idle_t \leq \delta_{low} \\ 0 & \text{when } Idle_t > \delta_{low} \end{cases}$$

When $Idle_t \geq \delta_{high}$, idle capacity is high, implying that supply elasticity at this time is high, and a shift of the demand curve has little effect on freight rates. When $Idle_t \leq \delta_{low}$, idle

TABLE 2 | Definitions of operating capacity indices.

Index	Explanation
Cap_A	Fronthaul capacity, in TEUs, on the shipping route from point O to point D in the previous 7 days.
Cap_B	Backhaul capacity, in TEUs, on the shipping route from point D to point O in the previous 7 days.
Cap_C	Total capacity of vessels, in TEUs, on the shipping route (sum of Cap_A and Cap_B).
Num_A	Fronthaul capacity, in number of vessels, on the shipping route from point O to point D in the previous 7 days.
Num_B	Backhaul capacity, in number of vessels, on the shipping route from point D to point O in the previous 7 days.
Num_C	The total number of vessels on a shipping route (sum of Num_A and Num_B).

capacity is low, implying that supply is inelastic and a small shift in the demand curve can cause a large change in freight rates. By cross-multiplying the two dummy variables with the operating capacity index, $Cap_{jt}^i \times Id_t^H$ and $Cap_{jt}^i \times Id_t^L$, we obtain the operating capacity under high and low idle capacity, respectively.

The shipping routes covered in Table 1 are components of the China Containerised Freight Index (CCFI), a broad index reflecting the trends of the global container market. CCFI freight rates measure the current freight rate for the fronthaul voyages and are based on transaction prices provided by 23 major Chinese and international shipping companies that have a significant market share on each route. Freight rates include freight charges and related surcharges and are therefore inclusive of all costs a shipper would be expected to pay.⁶ Finally, we use control variables to proxy for exogenous demand and supply shocks. These include the size of the fleet (supply factor), the total value of China's exports (demand factor) and the spot price of bunker fuel oil (cost factor).

Freight rates, China's total export values and fuel oil prices are obtained from the iFind database. The fleet size and idle capacity of the container shipping market are obtained from Clarkson's Shipping Intelligence Network. Except for the total value of exports and fleet size, which are measured monthly, all other variables are measured weekly. The time span of the data is from January 2014 to May 2023. See Table 3 for variable definitions and data sources.

Figure 3 shows the fronthaul operating capacity index, Cap_A , and the logarithmic freight rate changes for each route. Correlation analysis between previous periods' operating capacity ($Cap_{A,t-1}^i$, $Cap_{B,t-1}^i$ and $Cap_{C,t-1}^i$), current freight rate returns (Fre_t^i) and current idle capacity ($Idle_t$) for each of the nine shipping routes (in Table A1) indicates that there is no apparent linear relationship between the freight rate index,

TABLE 3 | Summary of variables.

Type	Variable	Definition	Measurement unit	Data source	Frequency of data
Dependent variable	Fre^i	Logarithmic returns of freight indices	—	iFind	Weekly
Explanatory variables	Cap_j^i	Operating capacity indices	TEUs	Calculated using AIS data	Weekly
	$Cap_j^i \times Id^H$	Operating capacity under high idle capacity	TEUs	Calculated using AIS data	Weekly
	$Cap_j^i \times Id^L$	Operating capacity under low idle capacity	TEUs	Calculated using AIS data	Weekly
Control variables	Fleet	Containership fleet	Thousands of TEUs	Clarkson's Shipping Intelligence Network	Monthly
	Export	Total value of China's exports	Hundreds of millions of US Dollars	iFind	Monthly
	Fuel	Logarithmic returns of 380 centistoke (cst) bunker heavy fuel oil	—	iFind	Weekly
Other variables	Idle	Containership idle capacity	TEUs	Clarkson's Shipping Intelligence Network	Weekly

Note: $i = 1, \dots, 9$ in variables Fre^i and Cap_j^i denote the Japan route, Europe route, U.S. West route, U.S. East route, Korea route, Southeast Asia route, Australia/New Zealand route, South Africa route and South America route, respectively. $j = A, B, C$ denote, respectively, fronthaul (Cap_A), backhaul (Cap_B) and total capacity (Cap_C).

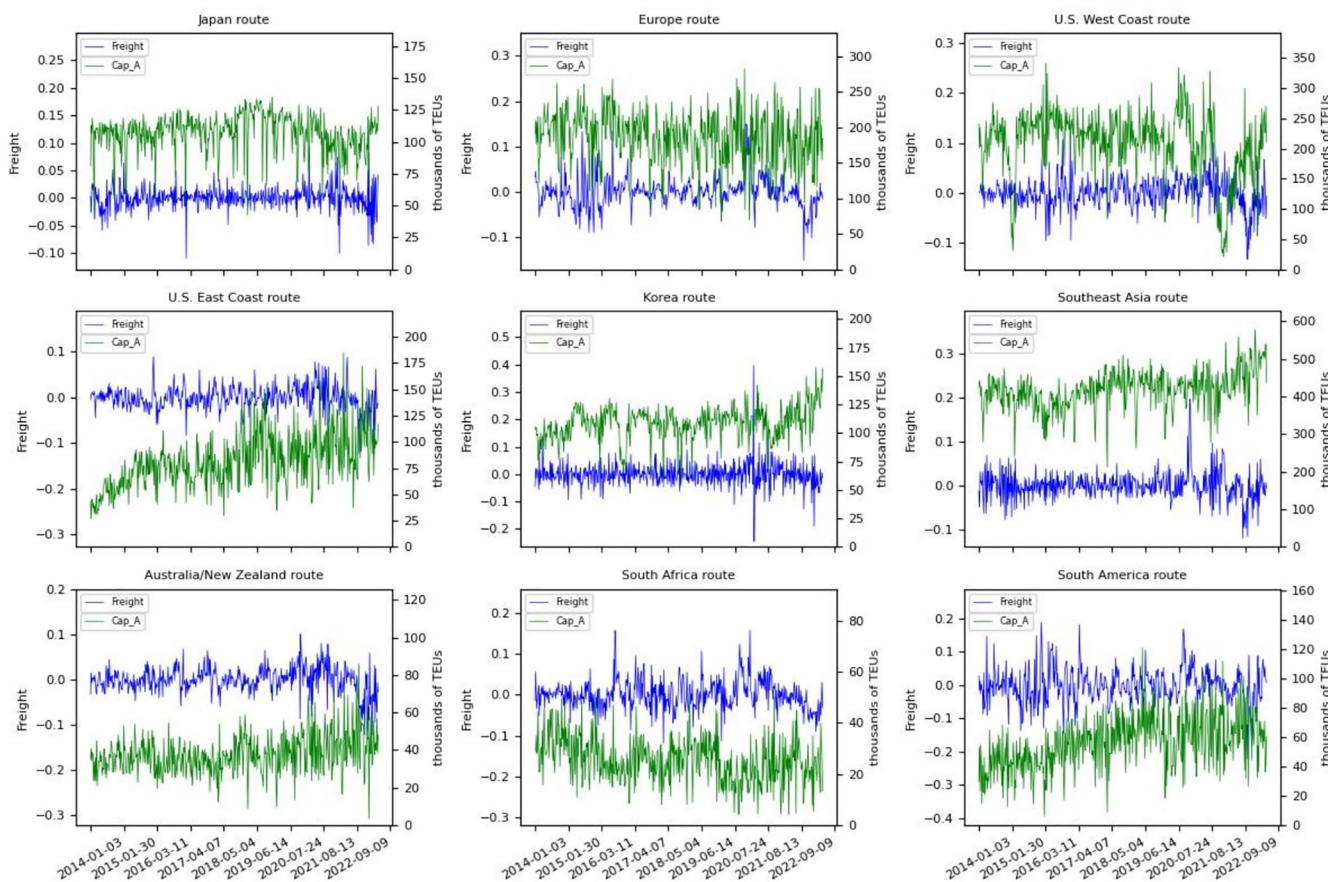


FIGURE 3 | Fronthaul operating capacity index and logarithmic freight rate returns. [Colour figure can be viewed at [wileyonlinelibrary.com](https://onlinelibrary.wiley.com)]

TABLE 4 | Granger causality tests of operating capacity and freight rates.

	Fre ¹	Fre ²	Fre ³	Fre ⁴	Fre ⁵	Fre ⁶	Fre ⁷	Fre ⁸	Fre ⁹
Panel A: Granger Causality test of operating capacity index to freight rate									
Cap _A ⁱ	0.651 (0.522)	2.754* (0.065)	3.222* (0.073)	0.228 (0.877)	5.201*** (0.006)	1.372 (0.251)	7.680*** (0.006)	2.412* (0.066)	3.364** (0.035)
Cap _B ⁱ	1.372 (0.255)	1.312 (0.253)	14.769*** (0.000)	3.222* (0.073)	6.822*** (0.001)	0.258 (0.855)	4.489** (0.035)	3.082** (0.016)	0.938 (0.422)
Cap _C ⁱ	0.048 (0.953)	0.910 (0.403)	12.504*** (0.000)	0.947 (0.389)	5.630*** (0.004)	1.133 (0.335)	11.954*** (0.001)	0.288 (0.592)	3.523* (0.061)
Panel B: Granger Causality test of freight rate to operational capacity index									
Cap _A ⁱ	1.055 (0.349)	2.896* (0.056)	0.175 (0.676)	1.222 (0.301)	1.342 (0.262)	0.591 (0.621)	0.107 (0.744)	2.168* (0.091)	3.109** (0.046)
Cap _B ⁱ	0.566 (0.568)	2.221 (0.137)	2.762* (0.097)	0.625 (0.430)	4.238** (0.015)	2.703** (0.045)	13.944*** (0.000)	1.737 (0.141)	0.571 (0.634)
Cap _C ⁱ	0.523 (0.593)	1.229 (0.294)	0.829 (0.363)	0.280 (0.756)	2.979* (0.052)	1.575 (0.195)	8.327*** (0.004)	0.021 (0.885)	0.436 (0.510)

Note: Granger causality tests of Cap_Aⁱ and Freⁱ have 2, 2, 1, 3, 2, 3, 1, 3 and 2 lags, respectively. Granger causality tests of Cap_Bⁱ and Freⁱ have 2, 1, 1, 1, 2, 3, 1, 4 and 3 lags, respectively. Granger causality tests of Cap_Cⁱ and Freⁱ have 2, 2, 1, 2, 2, 3, 1, 1 and 1 lag, respectively. $i = 1, \dots, 9$ denotes the Japan, Europe, U.S. West Coast, U.S. East Coast, Korea, Southeast Asia, Australia/New Zealand, South Africa and South America routes, respectively. The top value in each cell is the chi-square statistic χ^2 . p -values are in brackets. ***, ** and * indicate significance at the 1%, 5% and 10% level, respectively.

idle capacity and the operating capacity index. The empirical results later in this paper also show that the effect of the operating capacity index on the freight index is nonlinear and depends on idle capacity.

4 | Predictability of Operating Capacity on Freight Rate

4.1 | Operating Capacity and Freight Rates

We use Granger causality tests to examine the causal relationship between freight rates and operating capacity, and the results are presented in Table 4. Panel A presents the Granger causality test results for the impact of operating capacity index on freight rates, while Panel B shows the Granger causality tests for the effect of freight rates on operating capacity.

We note that the fronthaul capacity indices, Cap_Aⁱ, for the Europe (route 2), U.S. West Coast (route 3), Korea (route 5), Australia/New Zealand (route 7), South Africa (route 8) and South America (route 9) routes Granger-cause the corresponding freight rates. Conversely, only for the Europe (route 2), South African (route 8) and South American (route 9) routes, freight rates Granger-cause the corresponding operating capacity indices. The results for backhaul and total operating capacity indices Cap_Bⁱ and Cap_Cⁱ are similar to those for Cap_Aⁱ. In general, the capacity index appears to have a stronger predictive effect on freight rates rather than the other way around.

We test the predictive impact of operating capacity indices on the corresponding shipping freight rates more formally using the following regression model.

$$\text{Fre}_t^i = \alpha_0 + \alpha_1 \text{Cap}_{j,t-1}^i + \alpha_2 \text{Fre}_{t-1}^i + \varepsilon_t^i \quad (1)$$

The regression results for the fronthaul, backhaul and total operating capacity indices, Cap_Aⁱ, Cap_Bⁱ and Cap_Cⁱ, are presented in Panels A, B and C in Table A2, respectively.

The coefficients of the operating capacity indices for the nine shipping routes are positive or negative, although in most cases, their predictive effect on freight rates is not significant. Results remain qualitatively similar after we introduce control variables, including fleet size, the total value of China's exports and the spot price of fuel oil (regression results are in Table A3).

We also test the predictive effect of the operating capacity index on freight rates using a panel regression model.

$$\text{Fre}_t = \alpha_0 + \alpha_1 \text{Cap}_{j,t-1} + \alpha_2 \text{Fre}_{t-1} + \varepsilon_t \quad (2)$$

where $\text{Fre}_t = [\text{Fre}_t^1, \dots, \text{Fre}_t^9]^T$, $\text{Cap}_{j,t-1} = [\text{Cap}_{j,t-1}^1, \dots, \text{Cap}_{j,t-1}^9]^T$ and $\varepsilon_t = [\varepsilon_t^1, \dots, \varepsilon_t^9]^T$.

The regression results are presented in Table 5, where Columns (1), (3) and (5) show the baseline results, and Columns (2), (4) and (6) show the results incorporating control variables.

Consistent with the results from the individual regressions, the coefficients of the operating capacity indices (i.e., Cap_Aⁱ, Cap_Bⁱ and Cap_Cⁱ) are not significant in the panel data model. Therefore, univariate and panel regressions indicate that there is no significant linear predictability from the operating capacity index to freight rates.

TABLE 5 | Panel regressions of freight rates on operating capacity.

	Panel A: Fronthaul capacity index Cap_A		Panel B: Backhaul capacity index Cap_B		Panel C: Total capacity index Cap_C	
	(1)	(2)	(3)	(4)	(5)	(6)
Cap_{t-1}	0.134 (0.546)	0.128 (0.553)	0.024 (0.061)	0.082 (0.209)	0.073 (0.362)	0.091 (0.460)
$Fleet_t$		-0.115*** (-4.294)		-0.116*** (-4.446)		-0.117*** (-4.439)
$Export_t$		0.502*** (4.364)		0.509*** (4.296)		0.504*** (4.216)
$Fuel_t$		0.019** (2.055)		0.019** (2.062)		0.019** (2.062)
Fre_{t-1}	0.181 (1.484)	0.177 (1.452)	0.181 (1.483)	0.177 (1.450)	0.181 (1.484)	0.177 (1.451)
R^2	0.033	0.037	0.033	0.037	0.033	0.037

Note: Panel regressions of freight rates (in logarithmic returns) on operating capacity indices for the nine shipping routes. Columns (1), (3) and (5) show the results of the baseline regression. Columns (2), (4) and (6) are the regression results incorporating control variables. t -statistics using clustered standard errors are in brackets. ***, ** and * indicate significance at the 1%, 5% and 10% levels, respectively.

4.2 | Predictability Conditional on Supply Elasticity

We examine next the predictive effect of operating capacity conditional on different levels of supply elasticity. We set the idle capacity thresholds, δ_{high} and δ_{low} , as the 70th and 30th percentile of idle capacity, and obtain two explanatory variables, $Cap_{j,t}^i \times Id_t^H$ and $Cap_{j,t}^i \times Id_t^L$, representing operating capacity under high and low levels of supply elasticity, respectively. We use the following model to test the predictive effect of operating capacity on freight rates conditional on supply elasticity for the nine shipping routes.

$$Fre_t^i = \alpha_0 + \alpha_1 Cap_{j,t-1}^i + \alpha_2 Cap_{j,t-1}^i \times Id_{t-1}^H + \alpha_3 Cap_{j,t-1}^i \times Id_{t-1}^L + \alpha_4 Fre_{t-1}^i + \varepsilon_t^i \quad (3)$$

where $i = 1, \dots, 9$ denotes the nine routes as described above.

Two conclusions can be drawn from the regression results in Table 6. First, the regression coefficients of $Cap \times Id^H$ are in all cases negative. This indicates that when there is excess idle capacity (and supply elasticity is high), a reduction in operating capacity leads to higher freight rates. The results are statistically significant for the fronthaul index, Cap_A , in 3 shipping routes, for the backhaul index, Cap_B , in 1 shipping route, and for the total index, Cap_C , in 5 shipping routes. Second, the regression coefficients of $Cap \times Id^L$ are mostly positive although their impact on freight rates is insignificant in all cases. The influence of operating capacity on freight rates, conditional on supply elasticity, is also confirmed using the panel regression model.

$$Fre_t = \alpha_0 + \alpha_1 Cap_{j,t-1} + \alpha_2 Cap_{j,t-1} \times Id_{t-1}^H + \alpha_3 Cap_{j,t-1} \times Id_{t-1}^L + \alpha_4 Fre_{t-1} + \varepsilon_t \quad (4)$$

The results in Table 7 further confirm that the impact of operating capacity on freight rates varies depending on supply elasticity. When supply is elastic the regression coefficients of the operating capacity indices, $Cap_{j,t-1} \times Id_{t-1}^H$ in Equation (4), are significantly negative and when supply is inelastic, $Cap_{j,t-1} \times Id_{t-1}^L$ in Equation (4), the coefficient estimates are significantly positive. The results are consistent across the fronthaul, backhaul and total capacity indices and remain so after control variables have been included in the regression.

An important finding of this paper is that operating capacity can have the opposite impact on freight rates conditional on the level of idle capacity. Container shipping companies often switch from price competition—that is, competing on the freight rate they charge their customers—to quantity competition—that is, increasing their capacity to increase their market share and exploit economies of scale (Tvedt and Hovi 2024). Typically, they deploy larger and more efficient vessels on the mainline shipping routes that connect major ports around the world and have the larger volume of cargo flows. These are the routes that cover East–West trades such as the Europe, US West Coast and US East Coast routes. Similarly, they deploy smaller and less efficient vessels on regional trades (such as Japan and South Korea routes) or on trades with lower trading volumes.

The empirical results in the paper suggest that container shipping companies adjust their capacity according to existing competition and market dynamics as these are proxied by the elasticity of supply. For instance, a decision to reduce capacity on a route is more likely to occur when excess capacity is high (Cariou and Guillotreau 2022). By reducing their capacity in periods when there is excess capacity (and supply is elastic), shipping companies aim to increase their profits since the increase in freight rates outpaces the reduction in capacity due to the low elasticity

TABLE 6 | OLS regressions of freight rates on conditional operating capacity.

	(1)	(2)	(3)	(4)	(5)	(6)	(7)	(8)	(9)
	Fre ¹	Fre ²	Fre ³	Fre ⁴	Fre ⁵	Fre ⁶	Fre ⁷	Fre ⁸	Fre ⁹
Panel A: Fronthaul operating capacity index Cap _A									
Cap _{A,t-1}	0.120 (0.144)	0.870** (2.116)	0.522 (1.626)	-0.204 (-0.334)	-1.487 (-1.173)	-0.425 (-1.340)	-2.980 (-1.566)	0.349 (0.148)	-1.904 (-1.526)
Cap _{A,t-1} × Id _{t-1} ^H	-0.152 (-0.657)	-0.148 (-0.946)	-0.266 (-1.585)	-0.545 (-1.472)	-0.786* (-1.839)	-0.145 (-1.367)	-1.623* (-1.701)	-2.369 (-1.356)	-1.522 (-1.526)
Cap _{A,t-1} × Id _{t-1} ^L	-0.120 (-0.511)	-0.049 (-0.355)	0.076 (0.555)	0.443 (1.296)	-0.196 (-0.533)	0.110 (1.532)	0.335 (0.426)	0.691 (0.576)	0.105 (0.124)
Fre _{t-1}	-0.298*** (-3.945)	0.549*** (7.823)	0.179* (1.811)	0.255*** (3.244)	-0.366*** (-8.230)	0.059 (0.409)	0.222*** (3.224)	0.259*** (3.231)	0.434*** (7.597)
R ²	0.082	0.317	0.046	0.083	0.133	0.014	0.073	0.074	0.192
Panel B: Backhaul capacity index Cap _B									
Cap _{B,t-1}	-0.038 (-0.052)	-0.401 (-1.078)	1.246** (2.575)	0.809 (1.086)	-3.989*** (-2.813)	-0.240 (-0.570)	-2.412* (-1.922)	-1.290 (-1.168)	-1.176 (-0.704)
Cap _{B,t-1} × Id _{t-1} ^H	-0.144 (-0.640)	-0.203 (-0.957)	-0.260 (-1.307)	-0.396 (-0.634)	-0.515 (-1.470)	-0.192 (-1.470)	-0.898 (-1.155)	-2.178 (-1.455)	-2.481 (-1.519)
Cap _{B,t-1} × Id _{t-1} ^L	-0.098 (-0.430)	0.071 (0.350)	0.021 (0.162)	0.654 (1.190)	-0.115 (-0.365)	0.136 (1.619)	0.494 (0.700)	1.315 (1.066)	0.556 (0.357)
Fre _{t-1}	-0.298*** (-4.002)	0.551*** (8.744)	0.153* (1.668)	0.259*** (3.212)	-0.372*** (-8.485)	0.059 (0.412)	0.213*** (3.037)	0.251*** (3.140)	0.428*** (7.712)
R ²	0.081	0.311	0.064	0.081	0.150	0.014	0.061	0.080	0.189
Panel C: Total operating capacity index Cap _C									
Cap _{C,t-1}	0.015 (0.036)	0.268 (1.007)	0.713** (2.446)	0.167 (0.381)	-1.863** (-2.456)	-0.261 (-1.161)	-2.759** (-2.444)	-0.743 (-0.857)	-1.552 (-1.632)
Cap _{C,t-1} × Id _{t-1} ^H	-0.074 (-0.655)	-0.093 (-1.014)	-0.160* (-1.770)	-0.271 (-1.125)	-0.322* (-1.678)	-0.089 (-1.493)	-0.682* (-1.586)	-1.230 (-1.460)	-1.083* (-1.709)
Cap _{C,t-1} × Id _{t-1} ^L	-0.054 (-0.469)	-0.020 (-0.246)	-0.013 (-0.189)	0.277 (1.263)	-0.080 (-0.473)	0.062 (1.595)	0.148 (0.401)	0.589 (0.955)	0.062 (0.111)
Fre _{t-1}	-0.298*** (-3.975)	0.556*** (8.466)	0.164* (1.724)	0.259*** (3.270)	-0.370*** (-8.378)	0.058 (0.405)	0.211*** (3.154)	0.252*** (3.139)	0.434*** (7.739)
R ²	0.081	0.310	0.063	0.081	0.143	0.015	0.078	0.078	0.194

Note: OLS regressions of freight rates on conditional operating capacity using the model: $\text{Fre}_t^i = \alpha_0 + \alpha_1 \text{Cap}_{j,t-1}^i + \alpha_2 \text{Cap}_{j,t-1}^i \times \text{Id}_{t-1}^H + \alpha_3 \text{Cap}_{j,t-1}^i \times \text{Id}_{t-1}^L + \alpha_4 \text{Fre}_{t-1}^i + \epsilon_t^i$. When idle capacity is higher than the 70th percentile, $\text{Id}_t^H = 1$. When idle capacity is lower than the 30th percentile, $\text{Id}_t^L = 1$. In all other cases, the indicator is 0. *t*-statistics, using Newey-West HAC standard errors, are in brackets. ***, ** and * indicate significance at the 1%, 5% and 10% levels, respectively.

of demand. This is confirmed empirically by the negative sign of the conditional regression coefficients $\text{Cap}_{j,t-1}^i \times \text{Id}_{t-1}^H$ in Table 7.

On the other hand, when the supply curve is inelastic and the fleet is operating close to capacity, shipping companies can increase their short-run capacity in specific routes either by increasing the utilisation rate of the fleet—by increasing vessel speed—which results in higher fuel consumption and voyage

costs, or by rotating less efficient vessels—with higher operating costs—from other routes.⁷ Both measures will increase the marginal cost of transportation and result in higher transportation costs per unit of cargo. The empirical results in the paper confirm this conjecture in that increases in operating capacity when supply is inelastic will lead to significantly higher freight rates as confirmed by the positive sign of the conditional regression coefficients $\text{Cap}_{j,t-1}^i \times \text{Id}_{t-1}^L$ in Table 7.

TABLE 7 | Panel regressions of freight rates on conditional operating capacity.

	Panel A: Fronthaul capacity index Cap_A		Panel B: Backhaul capacity index Cap_B		Panel C: Total capacity index Cap_C	
	(1)	(2)	(3)	(4)	(5)	(6)
$Cap_{j,t-1}$	0.100 (0.341)	0.092 (0.326)	-0.105 (-0.278)	-0.052 (-0.139)	0.000 (0.001)	0.017 (0.078)
$Cap_{j,t-1} \times Id_{t-1}^H$	-0.201*** (-3.275)	-0.182*** (-3.006)	-0.281*** (-3.728)	-0.255*** (-3.467)	-0.119*** (-3.538)	-0.108*** (-3.264)
$Cap_{j,t-1} \times Id_{t-1}^L$	0.090*** (3.305)	0.095*** (3.713)	0.121*** (5.526)	0.127*** (5.110)	0.052*** (4.140)	0.055*** (4.199)
$Fleet_t$		-0.107*** (-4.087)		-0.104*** (-4.245)		-0.106*** (-4.208)
$Export_t$		0.459*** (3.853)		0.454*** (3.926)		0.458*** (3.744)
$Fuel_t$		0.020** (2.098)		0.020** (2.115)		0.020** (2.110)
Fre_{t-1}	0.176 (1.438)	0.173*** (1.411)	0.176 (1.434)	0.173 (1.407)	0.176 (1.435)	0.173 (1.408)
R^2	0.036	0.040	0.037	0.041	0.037	0.040

Note: Panel regressions of freight rates on conditional operating capacity using the model:

$Fre_t = \alpha_0 + \alpha_1 Cap_{j,t-1} + \alpha_2 Cap_{j,t-1} \times Id_{t-1}^H + \alpha_3 Cap_{j,t-1} \times Id_{t-1}^L + \alpha_4 Fre_{t-1} + \epsilon_t$. Columns (1), (3) and (5) show the results of the baseline regression. Columns (2), (4) and (6) are the regression results with control variables. When idle capacity is higher than the 70th percentile, $Id_t^H = 1$. When the idle capacity is lower than the 30th percentile, $Id_t^L = 1$. In all other cases, the indicator is 0. t -statistics, using clustered standard errors are in brackets. ***, ** and * indicate significance at the 1%, 5% and 10% levels, respectively.

The predictive ability of operating capacity, conditional on supply elasticity, is also confirmed by measuring the reduction in mean-squared prediction error (MSPE) using the out-of-sample R^2 , $R_{OS,M}^2$ (Gu et al. 2020; Bali et al. 2023). We divide the sample into a training sample τ_1 , to estimate the parameters of model M , and a test sample τ_2 , to test its predictive ability. $R_{OS,M}^2$ is calculated by evaluating the ability of model estimates, $\hat{r}_{i,t+1}^{(M)}$ to predict realised returns in the test sample period, as shown in formula (4).

$$R_{OS,M}^2 = 1 - \frac{\sum_{(i,t) \in \tau_2} (r_{i,t+1} - \hat{r}_{i,t+1}^{(M)})^2}{\sum_{(i,t) \in \tau_2} r_{i,t+1}^2} \quad (4)$$

We evaluate two models. Model 1 is the baseline model that includes only panel data with a one-period lag in freight rates. Model 2 is the conditional capacity model that includes operating capacity under different supply elasticities added to the baseline model. The R_{OS}^2 values of the two models for different test samples are presented in Table 8.

We can see that the $R_{OS,2}^2$ of Model 2 is greater than the $R_{OS,1}^2$ of Model 1, with a difference of almost 1.5 percentage points. This suggests that conditional operating capacity can predict freight rates and the prediction is very stable.

As additional supporting evidence for the predictive ability of the conditional capacity model over the baseline model we use the modified Diebold and Mariano (1995) (DM) and Clark and West (2007) (CW) tests. The modified DM test (Gu et al. 2020;

TABLE 8 | Comparison of out-of-sample predictability using R_{OS}^2 model.

	Cap_A	Cap_B	Cap_C
Panel A: test sample period of 0.5 year (December 2022–May 2023)			
$R_{OS,1}^2$	0.044	0.044	0.044
$R_{OS,2}^2$	0.059	0.062	0.061
Panel B: test sample period of 1.0 year (June 2022–May 2023)			
$R_{OS,1}^2$	0.076	0.076	0.076
$R_{OS,2}^2$	0.090	0.094	0.092
Panel C: test sample period of 1.5 years (December 2021–May 2023)			
$R_{OS,1}^2$	0.067	0.067	0.067
$R_{OS,2}^2$	0.080	0.084	0.082

Note: Out-of-sample R_{OS}^2 values for the baseline Model 1 and the conditional capacity Model 2. R_{OS}^2 is calculated using Equation (4). Panel A, Panel B and Panel C show the R_{OS}^2 values for the two models with test sample periods of 0.5 year (December 2022–May 2023), 1 year (June 2022–May 2023) and 1.5 years (December 2021–May 2023), respectively. Columns Cap_A , Cap_B and Cap_C represent the fronthaul, backhaul and total operating capacity indices.

Bali et al. 2023) considers the cross-sectional dependence in predictions and can accurately assess the out-of-sample predictive ability of panel models. Consider the mean-squared variance of

TABLE 9 | Diebold-Mariano and Clark-West tests for comparison of out-of-sample predictability.

	Model 2 (Cap _A)	Model 2 (Cap _B)	Model 2 (Cap _C)
Panel A: DM test			
Model 1 (0.5 year)	2.638***	2.322**	2.528***
Model 1 (1.0 year)	3.602***	3.415***	3.528***
Model 1 (1.5 years)	2.949***	2.709***	2.842***
Panel B: CW test			
Model 1 (0.5 year)	3.470***	3.011***	3.305***
Model 1 (1.0 years)	5.261***	5.194***	5.280***
Model 1 (1.5 years)	5.116***	4.915***	5.068***

Note: Diebold-Mariano (DM) (Panel A) and Clark-West (CW) (Panel B) test statistics for comparing out-of-sample predictive power of the baseline Model 1 and the conditional operating capacity Model 2. A positive number indicates that Model 2 outperforms Model 1. For each panel, the first, second and third rows correspond to test sample periods of 0.5 year (December 2022–May 2023), 1 year (June 2022–May 2023) and 1.5 years (December 2021–May 2023), respectively. The first, second and third columns correspond to fronthaul, backhaul and total operating capacity indices. ***, ** indicate significance at the 1% and 5% levels, respectively.

the prediction errors of Models 1 and 2 for the cross-section of panel data, $d_t^{(1,2)}$, in Equation (5):

$$d_{t+1}^{(1,2)} = \frac{1}{n_{\tau_2, t+1}} \sum_{i=1}^{n_{\tau_2, t+1}} \left[\left(\hat{e}_{i, t+1}^{(1)} \right)^2 - \left(\hat{e}_{i, t+1}^{(2)} \right)^2 \right] \quad (5)$$

The modified DM test statistic is calculated as:

$$DM^{(1,2)} = \frac{\bar{d}^{(1,2)}}{\hat{\sigma}_d^{(1,2)}} \quad (6)$$

where $\bar{d}^{(1,2)}$ and $\hat{\sigma}_d^{(1,2)}$ denote the mean and Newey-West (1987) standard error of $d_t^{(1,2)}$ over the testing sample.

The CW statistic compares the predictive accuracy for nested models by correcting the noise introduced in the estimation of additional parameters in the larger model (Model 2). Its null hypothesis (H_0) is that the predictive accuracy of the more parsimonious baseline model (Model 1) is no worse than that of the conditional capacity model (Model 2). The test eliminates estimation bias and constructs an asymptotically standard normal statistic using the difference in the MSPE of the two models. Rejection of the null indicates that the conditional capacity model has significantly better predictive performance than the baseline model.

As can be seen from Table 9, the statistics are all positive and significant at the 1% or 5% level. In other words, the conditional operating capacity model (Model 2) performs significantly better than the baseline model (Model 1) and results remain robust across different tests, different test samples, τ_2 , and different operating capacity indices.

5 | Robustness Checks

5.1 | Alternative Operating Capacity Indices Using Number of Ships

We use as alternative explanatory variables the operating capacity indices based on number of vessels operating on each shipping route, Num_A, Num_B and Num_C for the fronthaul, backhaul and

total operating indices, respectively. As can be seen from Table A4, when supply elasticity is high operating capacity has a significantly negative effect on next period's freight rates. On the other hand, at low levels of idle capacity (inelastic supply), operating capacity has a positive but insignificant effect on the freight rates. Therefore, results are qualitatively similar to those presented in Tables 6 and 7 but appear to be less significant in the case of inelastic supply. It should be noted however that indices based on number of ships do not measure accurately the increase in slot capacity since they put the same weight to a small containership of 3000 TEU and a large containership of 20,000 TEU.

5.2 | Using Average Vessel Speed as an Alternative Proxy for Capacity

An alternative measure of capacity utilisation is the average speed for each voyage. One expects that as idle capacity decreases and supply becomes inelastic, vessels will sail at higher speeds and thus average speed should have a positive correlation with freight rates. Conversely, when there is excess capacity, vessels will slow steam, and the correlation between average speed and freight rates should be negative. Therefore, we calculate an index that measures the average speed of each voyage as follows:

Step 1: Calculate the Actual Sailing Distance of Vessels for Each Route We identify trajectory points for each voyage using AIS data. The actual sailing distance is then obtained by summing the distances of the various trajectory segments along the route.

Step 2: Compute the Average Vessel Speed for Each Route By combining vessel departure and arrival timestamps at ports, the total voyage duration is determined, and the average speed per vessel–voyage is calculated. To construct daily time series for each ship, the voyage-averaged speed is mapped to the corresponding calendar days within the voyage period as daily speed observations.

Step 3: Calculate the Route-Level Average Speed The arithmetic mean of speeds across all vessels operating on that route on a given day.

Step 4: Generate Route-Specific Speed Index The speed index is the seven-day moving average of the route-level average speed for each of the nine shipping routes. As in the case of the operating capacity index, we construct a fronthaul weekly speed index, Spe_A , which represents the average speed in the direction from origin to destination and a backhaul speed index, Spe_B , which represents the average speed in the reverse direction (destination to origin).

We then carry out panel regressions of freight rates on the unconditional and conditional speed indices (i.e., under high and low supply elasticity), with and without controls. The regression results are presented in Table 10.

We observe that when supply elasticity is high (and idle capacity is low), voyage speed has a significantly negative impact on freight rates, whereas when supply elasticity is low, speed has a significantly positive impact on freight rates; overall, results are consistent with those presented for the operating capacity indices in Tables 6 and 7.

Furthermore, we use the product of speed with operating capacity indices to create a new composite indicator which accounts for both static carrying capacity and speed. Panel regression results, in Table 11, are entirely consistent with those derived from the capacity indices without considering speed. Therefore, from a robustness perspective, the operating capacity indices remain robust even after considering the impact of voyage speed.

5.3 | Alternative Definition for Idle Capacity

We also use an alternative measure for idle capacity that, in addition to idle containerships, also considers those that are in lay-up or undergoing repairs or scrubber retrofit. The results of the panel data regressions, presented in Table A5, remain robust for different levels of idle capacity. However, it should be noted that the significance of the regression coefficients decreases, which may be due to vessels under repair or in lay-up, just like newbuildings, not being immediately operational.

5.4 | Alternative Control Variables

In addition, we consider alternative control variables: China's total export value is replaced by China's Seaborne Containerised Exports,⁸ and the price of 380 centistoke (cst) heavy fuel oil is replaced by the price of 180 cst fuel oil. The results, in Table A6, remain qualitatively similar.

5.5 | Alternative Threshold Values for δ_{high} and δ_{low}

We consider different values for the two thresholds, δ_{high} and δ_{low} , which distinguish between different levels of supply elasticity. Specifically, we consider as thresholds the 60th and 40th percentiles, the 65th and 35th percentiles, the 75th and 25th

TABLE 10 | Panel regressions of freight rates on the conditional and unconditional speed indices.

	Panel A: Fronthaul speed index Spe_A				Panel B: Backhaul speed index Spe_B			
	(1)	(2)	(3)	(4)	(5)	(6)	(7)	(8)
$Spe_{j,t-1}$	3.780*** (9.299)	4.687*** (6.481)	3.395*** (7.871)	4.278*** (5.898)	2.607*** (5.663)	4.387*** (5.231)	2.380*** (5.260)	4.071*** (4.972)
$Spe_{j,t-1} \times Id_t^H$			-0.074*** (-5.374)	-0.066*** (-4.952)			-0.072*** (-5.979)	-0.061*** (-5.589)
$Spe_{j,t-1} \times Id_t^L$			0.036*** (2.783)	0.031*** (3.022)			0.049*** (3.372)	0.044*** (3.184)
$Fleet_t$		-0.186*** (-5.431)		-0.165*** (-5.359)		-0.223*** (-5.490)		-0.201*** (-5.298)
$Export_t$		0.600*** (5.530)		0.500*** (5.090)		0.481*** (3.890)		0.401*** (3.563)
$Fuel_t$		0.018** (2.015)		0.018** (2.090)		0.016* (1.729)		0.017* (1.832)
Fre_{t-1}	0.169 (1.398)	0.162 (1.335)	0.163 (1.343)	0.157 (1.293)	0.172 (1.414)	0.161 (1.321)	0.164 (1.353)	0.155 (1.276)
R^2	0.042	0.050	0.048	0.054	0.039	0.049	0.045	0.054

Note: Panel regressions of freight rates on conditional and unconditional speed index using the model:

$Fre_t = \alpha_0 + \alpha_1 Spe_{j,t-1} + \alpha_2 Spe_{j,t-1} \times Id_{t-1}^H + \alpha_3 Spe_{j,t-1} \times Id_{t-1}^L + \alpha_4 Fre_{t-1} + \epsilon_t$. Columns (1), (3), (5) and (7) show the results for the baseline regression. Columns (2), (4), (6) and (8) are the regression results after adding control variables. When idle capacity is higher than the 70th percentile, $Id_t^H = 1$. When idle capacity is lower than the 30th percentile, $Id_t^L = 1$. In all other cases, the indicator is 0. t -statistics, using clustered standard errors, are in brackets. ***, ** and * indicate significance at the 1%, 5% and 10% levels, respectively.

TABLE 11 | Panel regression of freight rates on combined speed and capacity indices.

	Panel A: Fronthaul composite index $\text{Spe}_A \times \text{Cap}_A$			Panel B: Backhaul composite index $\text{Spe}_B \times \text{Cap}_B$		
	(1)	(2)	(3)	(4)	(5)	(6)
$\text{Spe} \times \text{Cap}_{j,t-1}$	0.395 (1.491)	0.263 (0.932)	0.420 (1.278)	0.094 (0.297)	-0.051 (-0.168)	0.066 (0.184)
$\text{Spe} \times \text{Cap}_{j,t-1} \times \text{Id}_{t-1}^H$		-0.027*** (-6.582)	-0.025*** (-6.456)		-0.028*** (-6.837)	-0.025*** (-6.593)
$\text{Spe} \times \text{Cap}_{j,t-1} \times \text{Id}_{t-1}^L$		0.011*** (3.313)	0.011*** (3.376)		0.011*** (3.421)	0.012*** (3.926)
Fleet_t			-0.110*** (-5.830)			-0.099*** (-4.133)
Export_t			0.389*** (3.607)			0.392*** (3.408)
Fuel_t			0.020** (2.136)			0.020** (2.140)
Fre_{t-1}	0.180 (1.483)	0.172 (1.409)	0.169 (1.384)	0.181 (1.482)	0.172 (1.408)	0.169 (1.383)
R^2	0.033	0.041	0.044	0.033	0.040	0.043

Note: Panel regressions of freight rates on combined speed and capacity indices for different levels of idle capacity. Columns (1), (2), (4) and (5) show the results for the baseline regression. Columns (3) and (6) are the regression results after adding control variables. When idle capacity is higher than the 70th percentile, $\text{Id}_t^H = 1$. When idle capacity is lower than the 30th percentile, $\text{Id}_t^L = 1$. In all other cases, the indicator is 0. *t*-statistics, using clustered standard errors, are in brackets. ***, ** and * indicate significance at the 1%, 5% and 10% levels, respectively.

percentiles and the 80th and 20th percentiles of idle capacity, respectively. Results remain robust and the conditional operating capacity index can predict freight rates despite the use of different thresholds. Due to space limitations, the corresponding results are provided in the Tables A7–A10, respectively.

5.6 | Analysis With Monthly Data

Given that some of the control variables are only available at monthly frequency, we also estimate the regressions using monthly data. Regression results using monthly data are presented in Tables A11–A14 and are qualitatively similar to results using weekly data, indicating that changing the frequency of the data has no impact on the interpretation of the empirical results.

Concluding, the empirical results suggest that the impact of operating capacity on container freight rates depends on the level of idle capacity. When there is excess idle capacity and supply is elastic, reducing capacity can increase profits, as the resulting rise in freight rates outweighs the reduction in capacity. Conversely, when the container fleet operates near full capacity and supply is inelastic, increasing short-run capacity—either by speeding up vessels or redeploying less efficient ships—increases marginal costs and leads to higher freight rates. These findings suggest that shipping companies strategically adjust capacity based on market conditions to optimise profitability, shifting between price and quantity competition depending on route characteristics and supply elasticity.

6 | Conclusions

In this paper, we investigate the mechanism through which changes in operating capacity affect freight rates. We use AIS data to analyse the port calls and voyages of containerships from which we infer the operating capacity for individual shipping routes. We then apply the theories of supply elasticity and marginal cost to analyse their influence on container freight rates.

We show that, conditional on supply elasticity, operating capacity has predictive power on freight rates. Specifically, when the supply curve is inelastic and the fleet is operating close to full capacity, operating capacity has a positive effect on freight rates. We attribute this to increases in the marginal cost of transportation due to shipping companies' attempts to increase their short-run capacity on specific routes. In contrast, when the supply curve is elastic, operating capacity has a significantly negative effect on freight rates. This can be explained by the fact that a decision to reduce capacity on a route is more likely to occur when excess capacity is high. By reducing their capacity in periods of low utilisation, companies aim to increase their profits since the increase in freight rates outpaces the reduction in capacity due to the low elasticity of demand. The empirical results are robust to alternative specifications for the capacity indices, to changes in the average speed of the vessel, and to different specifications of how idle capacity is measured.

Acknowledgements

The paper has benefited from the helpful comments of two anonymous referees and the associate editor. We also want to thank participants at the 2025 Commodity Winter Workshops and the 2025 Commodity and Energy Association meetings for their valuable feedback. The authors gratefully acknowledge financial support from the National Natural Science Foundation of China (No. 72371045 and No. 71971034).

Conflicts of Interest

The authors declare no conflicts of interest.

Data Availability Statement

The data that support the findings of this study are available on request from the corresponding author. The data are not publicly available due to privacy or ethical restrictions.

Endnotes

¹ An example of how geopolitical uncertainty affects freight rates is the case of Houthi attacks on shipping traffic in the Red Sea in 2024, which has resulted in the rerouting of more than 60% of Europe-bound vessel traffic around the Cape of Good Hope. This has added more than 2 weeks on the duration of the average trip from SE Asia to Europe and has led to disruptions to global trade and a corresponding increase in freight rates; see as well Lloyd's List 5 September 2024: 'Red Sea reroutings uproot traditional transhipment trends'.

² Ocean-going containerships are equipped with AIS transponders that send satellite radio signals with geospatial information on vessel movements. Their primary use is for the safety of navigation and life at sea and for locating ships in search and rescue operations. The use of AIS transponders is mandatory for all vessels engaged in international voyages and weighing more than 300 tons.

³ Data from the United Nations Conference on Trade and Development Statistics (UNCTADstat).

⁴ The LSCI indicates an economy's position in the global container shipping network. It is based on the number of ship calls, the volume of containers handled in ports, the number of services and companies, the size of the largest ships, and the number of countries connected through direct shipping services. Data from UNCTADstat.

⁵ Idle status applies to containerships that have not been sailing with an average speed greater than one knot for 7 days or more, that have not been identified as being subject to another status (e.g., laid-up, under repair, in storage or similar), and have not subsequently recorded an average speed greater than one knot for two or more consecutive days or have not moved more than 20 nautical miles.

⁶ Freight rates for backhaul voyages are part of a counterpart freight index, the China Import Containerized Freight Index (CICFI) and are only available since 2022. Hence, are not included in the analysis presented here. Surcharges include Bunker/Fuel Adjustment Factor (BAF/FAF), Emergency Bunker Surcharges (EBS/EBA), Low Sulphur Fuel Surcharge (LSS), Currency Adjustment Factor/Yen Appreciation Surcharge (CAF/YAS), Peak Season Surcharge (PSS), War Risk Surcharge (WRS), Port Congestion Surcharge (PCS) and Canal Surcharge (SCS/SCF/PTF/PCC).

⁷ We focus on short-run adjustments since the total supply of shipping, that is, the stock of fleet, is fixed in the short-run. Ordering and building new ships will increase supply in the long-run. However, new orders will come in the market with a delay, given a lengthy construction lag (Kalouptsi 2014).

⁸ Data is from Clarkson's Shipping Intelligence Network and is monthly from January 2014 through May 2023.

References

- Alizadeh, A. H., and N. K. Nomikos. 2007. "Investment Timing and Trading Strategies in the Sale and Purchase Market for Ships." *Transportation Research Part B: Methodological* 41, no. 1: 126–143.
- Bali, T. G., H. Beckmeyer, M. Moerke, and F. Weigert. 2023. "Option Return Predictability With Machine Learning and Big Data." *Review of Financial Studies* 36, no. 9: 3548–3602.
- Bernhofen, D. M., Z. El-Sahli, and R. Kneller. 2016. "Estimating the Effects of the Container Revolution on World Trade." *Journal of International Economics* 98: 36–50.
- Boehm, C. E., and N. Pandalai-Nayar. 2022. "Convex Supply Curves." *American Economic Review* 112, no. 12: 3941–3969.
- Brancaccio, G., M. Kalouptsi, and T. Papageorgiou. 2020. "Geography, Transportation, and Endogenous Trade Costs." *Econometrica* 88, no. 2: 657–691.
- Cariou, P., and P. Guillotreau. 2022. "Capacity Management by Global Shipping Alliances: Findings From a Game Experiment." *Maritime Economics & Logistics* 24, no. 1: 41–66.
- Choi, T. M., S. H. Chung, and X. Zhuo. 2020. "Pricing With Risk Sensitive Competing Container Shipping Lines: Will Risk Seeking Do More Good Than Harm?" *Transportation Research Part B: Methodological* 133: 210–229.
- Clark, T. E., and K. D. West. 2007. "Approximately Normal Tests for Equal Predictive Accuracy in Nested Models." *Journal of Econometrics* 138, no. 1: 291–311.
- Coşar, A. K., and B. Demir. 2018. "Shipping Inside the Box: Containerization and Trade." *Journal of International Economics* 114: 331–345.
- Cullinane, K., and M. Khanna. 2000. "Economies of Scale in Large Containerships: Optimal Size and Geographical Implications." *Journal of Transport Geography* 8, no. 3: 181–195.
- Diebold, F. X., and R. S. Mariano. 1995. "Comparing Predictive Accuracy." *Journal of Business & Economic Statistics* 13, no. 3: 253–263.
- Drakos, K., and D. Tsouknidis. 2024. "Investment Under Uncertainty and Irreversibility: Evidence From the Shipping Markets." *International Journal of Finance and Economics* 29, no. 2: 2139–2154.
- Elmaghraby, W., and P. Keskinocak. 2003. "Dynamic Pricing in the Presence of Inventory Considerations: Research Overview, Current Practices, and Future Directions." *Management Science* 49, no. 10: 1287–1309.
- Finck, D., and P. Tillmann. 2022. "The Macroeconomic Effects of Global Supply Chain Disruptions." Technical Report, BOFIT Discussion Paper No. 14/2022.
- Gu, S., B. Kelly, and D. Xiu. 2020. "Empirical Asset Pricing via Machine Learning." *Review of Financial Studies* 33, no. 5: 2223–2273.
- Hummels, D. 2007. "Transportation Costs and International Trade in the Second Era of Globalization." *Journal of Economic Perspectives* 21, no. 3: 131–154.
- Kalouptsi, M. 2014. "Time to Build and Fluctuations in Bulk Shipping." *American Economic Review* 104, no. 2: 564–608.
- Kilian, L., N. K. Nomikos, and X. Zhou. 2023. "Container Trade and the US Recovery." *International Journal of Central Banking* 19, no. 1: 417–450.
- Koopmans, T. C. 1939. *Tanker Freight Rates and Tankship Building: An Analysis of Cyclical Fluctuations*. Haarlem-De Erven F Bohn NV.
- Li, L., Y. Wan, and D. Yang. 2024. "Do Shipping Alliances Affect Freight Rates? Evidence From Global Satellite Ship Data." *Transportation Research Part A: Policy and Practice* 181: 104010.
- Li, X., R. Zuidwijk, and M. B. M. de Koster. 2023. "Optimal Competitive Capacity Strategies: Evidence From the Container Shipping Market." *Omega* 115: 102790.

- Li, Y., X. Bai, Q. Wang, and Z. Ma. 2022. "A Big Data Approach to Cargo Type Prediction and Its Implications for Oil Trade Estimation." *Transportation Research Part E: Logistics and Transportation Review* 165: 102831.
- Michail, N. A., and K. D. Melas. 2021. "Sentiment-Augmented Supply and Demand Equations for the Dry Bulk Shipping Market." *Economies* 9, no. 4: 171.
- Nomikos, N. K., and D. A. Tsouknidis. 2022. "Disentangling Demand and Supply Shocks in the Shipping Freight Market: Their Impact on Shipping Investments." *Maritime Policy & Management* 50, no. 5: 563–581.
- Otani, S., and T. Matsuda. 2023. "Unified Container Shipping Industry Data From 1966: Freight Rate, Shipping Quantity, Newbuilding, Secondhand, and Scrap Price." *Transportation Research Part E: Logistics and Transportation Review* 176: 103186.
- Pascali, L. 2017. "The Wind of Change: Maritime Technology, Trade, and Economic Development." *American Economic Review* 107, no. 9: 2821–2854.
- Pouliasis, P. K., and C. Bentsos. 2024. "Oil Price Uncertainty and the Relation to Tanker Shipping." *International Journal of Finance and Economics* 29, no. 2: 2472–2494.
- Regli, F., and N. K. Nomikos. 2019. "The Eye in the Sky-Freight Rate Effects of Tanker Supply." *Transportation Research Part E: Logistics and Transportation Review* 125: 402–424.
- Saeed, N., and K. Cullinane. 2023. "Identifying the Characteristics of China's Maritime Trading Partners on the Basis of Bilateral Shipping Connectivity: A Cluster Analysis." *Maritime Policy & Management* 50, no. 1: 42–57.
- Song, C., and Y. Wang. 2022. "Slot Allocation and Exchange for Container Shipping Alliance Under Profit-Sharing Agreement and Uncertain Demand." *Ocean and Coastal Management* 229: 106335.
- Stopford, M. 2009. *Maritime Economics*. 3rd ed. Routledge.
- Tvedt, J., and I. B. Hovi. 2024. "Container Shipping: A Market Equilibrium Perspective on Freight Rates Formation Post-Covid-19." *Transportation Research Part A: Policy and Practice* 179: 103917.
- Wergeland, T. 1981. *Norbulk: A Simulation Model of Bulk Market Freight Rates*. Norwegian Norwegian School of Economics and Business Administration.
- Zheng, S., K. Wang, K. Dong, Y. Wan, and X. Fu. 2024. "Does the Shipping Alliance Aggravate or Alleviate Container Shipping Market Volatility." *Transportation Research Part A: Policy and Practice* 189: 104231.

Appendix A

TABLE A1 | Correlation analysis.

	Cap ¹ _{t-1}	Cap ² _{t-1}	Cap ³ _{t-1}	Cap ⁴ _{t-1}	Cap ⁵ _{t-1}	Cap ⁶ _{t-1}	Cap ⁷ _{t-1}	Cap ⁸ _{t-1}	Cap ⁹ _{t-1}
Panel A: Fronthaul operating capacity index Cap _A									
Fre ⁱ _t	0.015	0.146	0.082	-0.027	-0.046	-0.042	-0.131	-0.007	-0.037
Idle _t	-0.115	-0.069	-0.055	-0.090	-0.053	-0.320	0.030	-0.133	-0.213
Panel B: Backhaul operating capacity index Cap _B									
Fre ⁱ _t	0.005	-0.082	0.206	0.103	-0.130	0.003	-0.113	-0.049	-0.038
Idle _t	0.005	-0.125	-0.336	-0.147	0.111	-0.315	-0.017	-0.085	-0.043
Panel C: Total operating capacity index Cap _C									
Fre ⁱ _t	0.011	0.051	0.179	0.042	-0.102	-0.026	-0.172	-0.041	-0.048
Idle _t	-0.061	-0.137	-0.231	-0.147	0.036	-0.380	0.008	-0.134	-0.179

Note: Correlations between operating capacity (Capⁱ_{A,t-1}, Capⁱ_{B,t-1} and Capⁱ_{C,t-1}) at $t - 1$ and freight rate returns (Freⁱ_t) and idle capacity (Idle_t) for the nine shipping routes at t . $i = 1, \dots, 9$ denotes the Japan, Europe, U.S. West Coast, U.S. East Coast, Korea, Southeast Asia, Australia/New Zealand, South Africa and South America routes, respectively.

TABLE A2 | OLS regressions of freight rates on operating capacity.

	(1)	(2)	(3)	(4)	(5)	(6)	(7)	(8)	(9)
	Fre ¹	Fre ²	Fre ³	Fre ⁴	Fre ⁵	Fre ⁶	Fre ⁷	Fre ⁸	Fre ⁹
Panel A: Fronthaul operating capacity index Cap _A									
Cap _{A,t-1}	-0.018 (-0.022)	0.822** (1.970)	0.451 (1.584)	-0.099 (-0.177)	-1.834 (-1.436)	-0.263 (-0.904)	-3.409* (-1.684)	0.536 (0.233)	-1.992* (-1.863)
Fre _{t-1}	-0.298*** (-3.977)	0.551*** (7.832)	0.194* (1.946)	0.277*** (3.516)	-0.362*** (-8.345)	0.075 (0.515)	0.229*** (3.257)	0.274*** (3.519)	0.438*** (7.582)
R ²	0.084	0.319	0.040	0.073	0.130	0.003	0.065	0.071	0.189
Panel B: Backhaul operating capacity index Cap _B									
Cap _{B,t-1}	-0.158 (-0.211)	-0.418 (-1.185)	1.363*** (3.010)	0.958 (1.592)	-4.401*** (-3.137)	0.011 (0.027)	-2.506** (-1.995)	-1.142 (-1.102)	-1.704 (-1.073)
Fre _{t-1}	-0.299*** (-4.015)	0.556*** (8.895)	0.159* (1.746)	0.270*** (3.294)	-0.370*** (-8.591)	0.075 (0.519)	0.223*** (3.098)	0.271*** (3.451)	0.434*** (7.602)
R ²	0.084	0.312	0.063	0.079	0.150	0.001	0.059	0.072	0.187
Panel C: Total operating capacity index Cap _C									
Cap _{C,t-1}	-0.055 (-0.126)	0.240 (0.890)	0.692** (2.573)	0.276 (0.697)	-2.082*** (-2.725)	-0.108 (-0.537)	-2.921** (-2.464)	-0.510 (-0.601)	-1.613* (-1.771)
Fre _{t-1}	-0.298*** (-3.997)	0.559*** (8.468)	0.176* (1.844)	0.277** (3.443)	-0.367*** (-8.495)	0.075 (0.518)	0.219*** (3.205)	0.271*** (3.474)	0.439 (7.684)
R ²	0.084	0.312	0.059	0.074	0.142	0.002	0.073	0.071	0.190

Note: Regression model based on Equation (1), $Fre_t^i = \alpha_0 + \alpha_1 Cap_{j,t-1}^i + \alpha_2 Fre_{t-1}^i + \epsilon_t^i$. t -statistics using Newey-West HAC standard errors are in brackets. ***, ** and * indicate significance at the 1%, 5% and 10% levels, respectively.

TABLE A3 | Predictability of operating capacity on freight rates (with control variables).

	(1)	(2)	(3)	(4)	(5)	(6)	(7)	(8)	(9)
	Fre ¹	Fre ²	Fre ³	Fre ⁴	Fre ⁵	Fre ⁶	Fre ⁷	Fre ⁸	Fre ⁹
Panel A: operating capacity index Cap _A									
Cap _{t-1}	0.099 (0.153)	0.768** (2.194)	0.448* (1.724)	0.127 (0.230)	-1.726 (-1.259)	-0.427 (-1.316)	-3.539*** (-2.673)	-0.562 (-0.290)	-2.614* (-1.941)
Fleet _t	-0.000 (-0.003)	-0.081 (-0.994)	-0.055 (-0.644)	-0.114 (-1.432)	-0.202* (-1.705)	-0.171* (-1.850)	-0.115 (-1.437)	-0.179* (-1.680)	0.058 (0.408)
Export _t	0.217 (0.748)	0.613 (1.579)	0.253 (0.612)	0.419 (1.179)	1.057* (1.879)	1.084** (2.345)	0.582 (1.484)	0.684 (1.387)	0.254 (0.386)
Fuel _t	0.020 (1.263)	-0.038* (-1.782)	0.036 (1.564)	0.011 (0.567)	0.055* (1.767)	-0.020 (-0.809)	0.011 (0.528)	0.030 (1.134)	0.019 (0.507)
Fre _{t-1}	-0.297*** (-6.713)	0.552*** (14.474)	0.194*** (4.312)	0.275*** (6.190)	-0.366*** (-8.550)	0.070 (1.533)	0.223*** (4.997)	0.264*** (5.915)	0.439*** (10.541)
R ²	0.084	0.323	0.040	0.072	0.137	0.010	0.065	0.072	0.186
Panel B: operating capacity index Cap _B									
Cap _{t-1}	-0.097 (-0.150)	-0.368 (-1.004)	1.328*** (3.735)	1.353** (2.310)	-4.225*** (-3.420)	0.134 (0.317)	-2.320* (-1.930)	-2.411* (-1.689)	-2.560 (-1.424)
Fleet _t	0.001 (0.013)	-0.112 (-1.393)	-0.058 (-0.685)	-0.152** (-2.016)	-0.166 (-1.429)	-0.193* (-1.937)	-0.114 (-1.412)	-0.249** (-2.253)	0.042 (0.291)
Export _t	0.208 (0.715)	0.694* (1.787)	0.163 (0.401)	0.386 (1.092)	0.888 (1.589)	0.908** (2.026)	0.368 (0.953)	0.807* (1.646)	0.309 (0.466)
Fuel _t	0.020 (1.257)	-0.038* (-1.765)	0.032 (1.395)	0.012 (0.622)	0.056* (1.827)	-0.020 (-0.797)	0.016 (0.732)	0.026 (0.969)	0.016 (0.434)
Fre _{t-1}	-0.298*** (-6.731)	0.557*** (14.559)	0.160*** (3.512)	0.262*** (5.913)	-0.372*** (-8.790)	0.070 (1.527)	0.218*** (4.843)	0.260*** (5.852)	0.434*** (10.433)
R ²	0.084	0.318	0.062	0.082	0.155	0.007	0.058	0.078	0.183
Panel C: operating capacity index Cap _C									
Cap _{t-1}	0.000 (0.001)	0.217 (0.869)	0.693*** (3.455)	0.677* (1.715)	-2.030*** (-2.731)	-0.181 (-0.772)	-3.006*** (-3.320)	-1.715 (-1.512)	-2.937*** (-2.570)
Fleet _t	0.000 (0.004)	-0.117 (-1.466)	-0.043 (-0.509)	-0.167** (-2.059)	-0.166 (-1.403)	-0.161* (-1.678)	-0.092 (-1.150)	-0.258** (-2.224)	0.143 (0.957)
Export _t	0.213 (0.732)	0.726* (1.880)	0.286 (0.698)	0.383 (1.078)	0.974* (1.739)	1.009** (2.193)	0.533 (1.383)	0.850* (1.704)	0.409 (0.619)
Fuel _t	0.020 (1.255)	-0.037* (-1.712)	0.033 (1.459)	0.011 (0.573)	0.057* (1.824)	-0.020 (-0.803)	0.014 (0.671)	0.028 (1.034)	0.015 (0.418)
Fre _{t-1}	-0.298*** (-6.720)	0.558*** (14.609)	0.176*** (3.929)	0.271*** (6.121)	-0.370*** (-8.693)	0.071 (1.552)	0.214*** (4.796)	0.257*** (5.762)	0.442*** (10.637)
R ²	0.084	0.317	0.058	0.077	0.147	0.008	0.072	0.077	0.191

Note: Table A3 shows the results of regressing the freight indices on the operating capacity indices and the control variables for the nine shipping routes. The regression model uses the equation $Fre_t^i = \alpha_0 + \alpha_1 Cap_{t-1}^i + \alpha_2 Fre_{t-1}^i + \alpha_3 \mathbf{Control}_t + \varepsilon_t^i$. $\mathbf{Control} = [\text{Fleet}, \text{Export}, \text{Fuel}]^T$ represent the containership fleet, the total value of China's exports, and the logarithmic returns of spot prices of fuel oils, respectively. The t -statistics are in parentheses. ***, ** and * indicate significance at the 1%, 5% and 10% levels, respectively.

TABLE A4 | Panel regressions of freight rates on conditional operating capacity (with alternative operating capacity indices).

	Panel A: Fronthaul operating capacity index Num _A			Panel B: Backhaul operating capacity index Num _B			Panel C: Total operating capacity index Num _C		
	(1)	(2)	(3)	(4)	(5)	(6)	(7)	(8)	(9)
Cap _{t-1}	-0.004 (-0.819)	-0.004 (-0.785)	-0.006 (-1.111)	-0.006 (-0.908)	-0.006 (-1.117)	-0.006 (-1.110)	-0.003 (-1.039)	-0.003 (-1.192)	-0.004 (-1.394)
Cap _{t-1} × Id _{t-1} ^H		-0.005*** (-3.763)	-0.004*** (-3.462)		-0.006*** (-4.734)	-0.005*** (-4.396)		-0.003*** (-4.312)	-0.002*** (-3.987)
Cap _{t-1} × Id _{t-1} ^L		0.001 (1.228)	0.001 (1.383)		0.001 (1.168)	0.002 (1.294)		0.001 (1.242)	0.001 (1.381)
Fleet _t			-0.110*** (-4.267)			-0.107*** (-4.376)			-0.109*** (-4.323)
Export _t			0.490*** (3.913)			0.479*** (4.123)			0.488*** (3.986)
Fuel _t			0.019** (2.068)			0.019** (2.085)			0.019** (2.076)
Fre _{t-1}	0.181 (1.480)	0.178 (1.454)	0.175 (1.425)	0.181 (1.479)	0.178 (1.454)	0.175 (1.425)	0.181 (1.478)	0.178 (1.452)	0.175 (1.423)
R ²	0.033	0.035	0.038	0.033	0.035	0.039	0.033	0.035	0.039

Note: Panel regression results of freight rates on fronthaul (Num_A), backhaul (Num_B) and total (Num_C) alternative operating capacity indices, using the number of vessels in operation. Columns (1), (4) and (7) show the results of the baseline regression. Columns (2), (5) and (8) are the regression results with different levels of idle capacity. Columns (3), (6) and (9) are results with control variables. *t*-statistics using clustered standard errors are in brackets. *** and ** indicate significance at the 1% and 5% levels, respectively.

TABLE A5 | Panel regressions of freight rates on conditional operating capacity (with alternative measure of idle capacity).

	Panel A: Fronthaul operating capacity index Cap _A		Panel B: Backhaul operating capacity index Cap _B		Panel C: Total operating capacity index Cap _C	
	(1)	(2)	(3)	(4)	(5)	(6)
Cap _{t-1}	0.127 (0.488)	0.126 (0.519)	-0.006 (-0.015)	0.053 (0.143)	0.052 (0.251)	0.076 (0.372)
Cap _{t-1} × Id _{t-1} ^H	-0.119** (-2.242)	-0.086 (-1.608)	-0.176** (-2.490)	-0.135* (-1.958)	-0.072** (-2.333)	-0.054* (-1.745)
Cap _{t-1} × Id _{t-1} ^L	0.043 (1.545)	0.030 (1.127)	0.069** (2.233)	0.056* (1.860)	0.027** (2.011)	0.020 (1.569)
Fleet _t		-0.106*** (-4.026)		-0.103*** (-4.167)		-0.105*** (-4.181)
Export _t		0.452*** (3.859)		0.439*** (3.869)		0.445*** (3.746)
Fuel _t		0.019** (2.040)		0.019** (2.040)		0.019** (2.043)
Fre _{t-1}	0.179 (1.466)	0.177 (1.441)	0.179 (1.460)	0.176 (1.436)	0.179 (1.463)	0.176 (1.439)
R ²	0.034	0.037	0.035	0.038	0.034	0.037

Note: Panel regressions of freight rates on conditional operating capacity, with an alternative measure of idle capacity which also counts containerships that are laid up or enter ship repair yards for scrubber conversions. Columns (1), (3) and (5) show the results of the baseline regression. Columns (2), (4) and (6) are the regression results with control variables. *t*-statistics, using clustered standard errors, are in brackets. ***, ** and * indicate significance at the 1%, 5% and 10% levels, respectively.

TABLE A6 | Panel regressions of freight rates on conditional operating capacity (with alternative control variables).

	Panel A: Fronthaul operating capacity index Cap_A		Panel B: Backhaul operating capacity index Cap_B		Panel C: Total operating capacity index Cap_C	
	(1)	(2)	(3)	(4)	(5)	(6)
Cap_{t-1}	0.100 (0.341)	-0.031 (-0.103)	-0.105 (-0.278)	-0.104 (-0.269)	0.000 (0.001)	-0.063 (-0.263)
$Cap_{t-1} \times Id_{t-1}^H$	-0.201*** (-3.275)	-0.169*** (-3.063)	-0.281*** (-3.728)	-0.236*** (-3.444)	-0.119*** (-3.538)	-0.101*** (-3.369)
$Cap_{t-1} \times Id_{t-1}^L$	0.090*** (3.305)	0.072*** (2.772)	0.121*** (5.526)	0.096*** (4.704)	0.052*** (4.140)	0.043*** (3.529)
$Fleet_t$		-0.172*** (-7.998)		-0.168*** (-8.900)		-0.170*** (-8.314)
$Export_t$		0.001*** (6.771)		0.001*** (6.852)		0.001*** (6.399)
$Fuel_t$		0.019** (2.002)		0.020** (2.023)		0.020** (2.008)
Fre_{t-1}	0.176 (1.438)	0.166 (1.368)	0.176 (1.434)	0.166 (1.367)	0.176 (1.435)	0.166 (1.366)
R^2	0.036	0.047	0.037	0.048	0.037	0.048

Note: Panel regressions of freight rates on conditional operating capacity with alternative control variables. Export denotes China's Seaborne Containerised Exports, and Fuel denotes the logarithmic returns of the price of fuel oils (180). Columns (2), (4) and (6) show the regression results with alternative control variables. t -statistics, using clustered standard errors, are in brackets. *** and ** indicate significance at the 1% and 5% levels, respectively.

TABLE A7 | Panel regressions of freight rates on conditional operating capacity (with 60th and 40th percentile thresholds for idle capacity).

	Panel A: Fronthaul operating capacity index Cap_A		Panel B: Backhaul operating capacity index Cap_B		Panel C: Total operating capacity index Cap_C	
	(1)	(2)	(3)	(4)	(5)	(6)
Cap_{t-1}	0.024 (0.085)	0.011 (0.041)	-0.133 (-0.337)	-0.091 (-0.227)	-0.037 (-0.173)	-0.027 (-0.120)
$Cap_{t-1} \times Id_{t-1}^H$	-0.112 (-1.419)	-0.100 (-1.220)	-0.215** (-2.231)	-0.196** (-1.976)	-0.080* (-1.846)	-0.072 (-1.610)
$Cap_{t-1} \times Id_{t-1}^L$	0.167*** (5.743)	0.167*** (4.851)	0.157*** (3.471)	0.158*** (2.851)	0.083*** (4.423)	0.083*** (3.548)
$Fleet_t$		-0.102*** (-3.939)		-0.099*** (-4.131)		-0.101*** (-4.057)
$Export_t$		0.483*** (4.030)		0.472*** (4.091)		0.480*** (3.910)
$Fuel_t$		0.020** (2.113)		0.020** (2.130)		0.020** (2.127)
Fre_{t-1}	0.176 (1.438)	0.173 (1.411)	0.176 (1.440)	0.173 (1.413)	0.176 (1.438)	0.173 (1.411)
R^2	0.037	0.040	0.038	0.041	0.037	0.041

Note: When the idle capacity is higher than the 60th percentile, $Id_t^H = 1$. When the idle capacity is lower than the 40th percentile, $Id_t^L = 1$. In all other cases, the indicator is 0. Columns (1), (3) and (5) show the regression results at different levels of idle capacity. Columns (2), (4) and (6) are results with control variables. t -statistics, using clustered standard errors, are in brackets. ***, ** and * indicate significance at the 1%, 5% and 10% levels, respectively.

TABLE A8 | Panel regressions of freight rates on conditional operating capacity (with 65th and 35th percentile thresholds for idle capacity).

	Panel A: Fronthaul operating capacity index Cap_A		Panel B: Backhaul operating capacity index Cap_B		Panel C: Total operating capacity index Cap_C	
	(1)	(2)	(3)	(4)	(5)	(6)
Cap_{t-1}	0.086 (0.315)	0.074 (0.284)	-0.098 (-0.256)	-0.049 (-0.126)	-0.004 (-0.019)	0.011 (0.051)
$Cap_{t-1} \times Id_{t-1}^H$	-0.162*** (-3.654)	-0.141*** (-3.212)	-0.262*** (-4.482)	-0.232*** (-4.019)	-0.104*** (-4.322)	-0.091*** (-3.803)
$Cap_{t-1} \times Id_{t-1}^L$	0.094*** (3.121)	0.101*** (3.155)	0.100*** (2.938)	0.109*** (2.655)	0.049*** (3.091)	0.053*** (2.882)
$Fleet_t$		-0.107*** (-4.086)		-0.103*** (-4.224)		-0.105*** (-4.200)
$Export_t$		0.468*** (4.062)		0.452*** (3.937)		0.462*** (3.849)
$Fuel_t$		0.020** (2.113)		0.020** (2.123)		0.020** (2.123)
Fre_{t-1}	0.176 (1.441)	0.173 (1.413)	0.176 (1.436)	0.173 (1.409)	0.176 (1.437)	0.173 (1.411)
R^2	0.036	0.039	0.037	0.040	0.036	0.040

Note: When the idle capacity is higher than the 65th percentile, $Id_t^H = 1$. When the idle capacity is lower than the 35th percentile, $Id_t^L = 1$. In all other cases, the indicator is 0. Columns (1), (3) and (5) show the regression results at different levels of idle capacity. Columns (2), (4) and (6) are results with control variables. t -statistics, using clustered standard errors, are in brackets. *** and ** indicate significance at the 1% and 5% levels, respectively.

TABLE A9 | Panel regressions of freight rates on conditional operating capacity (with 75th and 25th percentile thresholds for idle capacity).

	Panel A: Fronthaul operating capacity index Cap_A		Panel B: Backhaul operating capacity index Cap_B		Panel C: Total operating capacity index Cap_C	
	(1)	(2)	(3)	(4)	(5)	(6)
Cap_{t-1}	0.133 (0.461)	0.132 (0.481)	-0.058 (-0.151)	0.002 (0.006)	0.026 (0.114)	0.049 (0.217)
$Cap_{t-1} \times Id_{t-1}^H$	-0.256*** (-3.900)	-0.230*** (-3.785)	-0.351*** (-4.246)	-0.319*** (-4.105)	-0.150*** (-4.034)	-0.136*** (-3.914)
$Cap_{t-1} \times Id_{t-1}^L$	0.027 (1.206)	0.025 (1.242)	0.053** (2.450)	0.050** (2.284)	0.019* (1.782)	0.017* (1.718)
$Fleet_t$		-0.104*** (-4.072)		-0.101*** (-4.236)		-0.103*** (-4.216)
$Export_t$		0.433*** (3.863)		0.428*** (3.926)		0.431*** (3.745)
$Fuel_t$		0.019** (2.021)		0.019** (2.026)		0.019** (2.027)
Fre_{t-1}	0.176 (1.435)	0.174 (1.412)	0.175 (1.427)	0.173 (1.404)	0.176 (1.430)	0.173 (1.407)
R^2	0.036	0.039	0.037	0.040	0.037	0.040

Note: When the idle capacity is higher than the 75th percentile, $Id_t^H = 1$. When the idle capacity is lower than the 25th percentile, $Id_t^L = 1$. In all other cases, the indicator is 0. Columns (1), (3) and (5) show the regression results at different levels of idle capacity. Columns (2), (4) and (6) are results with control variables. t -statistics, using clustered standard errors, are in brackets. ***, ** and * indicate significance at the 1%, 5% and 10% levels, respectively.

TABLE A10 | Panel regressions of freight rates on conditional operating capacity (with 80th and 20th percentile thresholds for idle capacity).

	Panel A: Fronthaul operating capacity index Cap_A		Panel B: Backhaul operating capacity index Cap_B		Panel C: Total operating capacity index Cap_C	
	(1)	(2)	(3)	(4)	(5)	(6)
Cap_{t-1}	0.110 (0.392)	0.110 (0.413)	-0.059 (-0.154)	0.003 (0.009)	0.021 (0.091)	0.044 (0.201)
$Cap_{t-1} \times Id_{t-1}^H$	-0.228*** (-3.314)	-0.204*** (-3.133)	-0.319*** (-3.601)	-0.289*** (-3.398)	-0.135*** (-3.417)	-0.122*** (-3.237)
$Cap_{t-1} \times Id_{t-1}^L$	0.054** (2.051)	0.049** (2.026)	0.078*** (2.906)	0.071*** (2.787)	0.033** (2.440)	0.029** (2.311)
$Fleet_t$		-0.107*** (-4.123)		-0.105*** (-4.280)		-0.107*** (-4.259)
$Export_t$		0.452*** (3.941)		0.449*** (4.015)		0.451*** (3.841)
$Fuel_t$		0.019** (2.016)		0.019** (2.019)		0.019** (2.020)
Fre_{t-1}	0.178 (1.453)	0.175 (1.426)	0.177 (1.447)	0.175 (1.421)	0.177 (1.450)	0.175 (1.424)
R^2	0.035	0.039	0.036	0.039	0.036	0.039

Note: When the idle capacity is higher than the 80th percentile, $Id_t^H = 1$. When the idle capacity is lower than the 20th percentile, $Id_t^L = 1$. In all other cases, the indicator is 0. Columns (1), (3) and (5) show the regression results at different levels of idle capacity. Columns (2), (4) and (6) are results with control variables. t -statistics, using clustered standard errors, are in brackets. *** and ** indicate significance at the 1% and 5% levels, respectively.

TABLE A11 | Predictability of operating capacity on freight rates (monthly data).

	(1)	(2)	(3)	(4)	(5)	(6)	(7)	(8)	(9)
	Fre ¹	Fre ²	Fre ³	Fre ⁴	Fre ⁵	Fre ⁶	Fre ⁷	Fre ⁸	Fre ⁹
Panel A: Fronthaul operating capacity index Cap _A									
Cap _{A,t-1}	1.085 (0.467)	-2.866 (-0.985)	-0.355 (-0.244)	-2.086 (-0.734)	-8.436** (-2.424)	-1.127 (-0.632)	-2.685 (-0.313)	1.017 (0.080)	10.079 (1.125)
Fre _{t-1}	0.284** (2.381)	0.492*** (4.436)	0.372*** (2.609)	0.201 (1.555)	0.313** (2.186)	0.338*** (2.867)	0.577*** (5.510)	0.495*** (6.946)	0.119 (1.535)
R ²	0.065	0.230	0.122	0.029	0.126	0.109	0.322	0.223	0.011
Panel B: Backhaul operating capacity index Cap _B									
Cap _{B,t-1}	-1.414 (-0.632)	-0.924 (-0.557)	2.564* (1.773)	1.299 (0.293)	-9.377*** (-2.673)	-1.184 (-0.636)	-7.199 (-1.015)	5.040 (0.760)	-2.685 (-0.307)
Fre _{t-1}	0.270** (2.088)	0.477*** (4.311)	0.334** (2.401)	0.202 (1.478)	0.288** (2.125)	0.351*** (3.016)	0.565*** (5.714)	0.500*** (7.080)	0.127 (1.465)
R ²	0.066	0.222	0.136	0.026	0.147	0.108	0.330	0.227	-0.001
Panel C: Total operating capacity index Cap _C									
Cap _{C,t-1}	-0.070 (-0.054)	-1.773 (-1.073)	0.646 (0.538)	-0.510 (-0.229)	-5.964*** (-2.909)	-0.882 (-0.695)	-4.812 (-0.802)	3.435 (0.906)	4.332 (0.681)
Fre _{t-1}	0.278** (2.249)	0.479*** (4.448)	0.361** (2.411)	0.205 (1.549)	0.292** (2.165)	0.342*** (2.899)	0.564*** (5.769)	0.501*** (7.096)	0.127 (1.556)
R ²	0.063	0.228	0.124	0.025	0.152	0.110	0.329	0.226	0.003

Note: Regression model based on Equation (1), $Fre_t^i = \alpha_0 + \alpha_1 Cap_{j,t-1}^i + \alpha_2 Fre_{t-1}^i + \varepsilon_t^i$, t -statistics, using Newey-West HAC standard errors, are in brackets. *** and ** indicate significance at the 1% and 5% levels, respectively.

TABLE A12 | Panel regressions of freight rates on operating capacity (monthly data).

	Panel A: Fronthaul capacity index Cap _A		Panel B: Backhaul capacity index Cap _B		Panel C: Total operating capacity index Cap _C	
	(1)	(2)	(3)	(4)	(5)	(6)
Cap _{t-1}	-0.847* (-1.671)	-0.738 (-1.387)	-0.359 (-0.358)	-0.173 (-0.178)	-0.559 (-1.073)	-0.445 (-0.840)
Fleet _t		-0.118 (-1.528)		-0.122* (-1.677)		-0.113 (-1.574)
Export _t		0.093 (0.204)		0.076 (0.169)		0.094 (0.207)
Fuel _t		0.055*** (3.169)		0.055*** (3.229)		0.055*** (3.184)
Fre _{t-1}	0.323*** (4.303)	0.320*** (4.314)	0.323*** (4.291)	0.321*** (4.302)	0.323*** (4.300)	0.321*** (4.309)
R ²	0.104	0.111	0.104	0.110	0.104	0.110

Note: Panel regressions of freight rates (in logarithmic returns) on operating capacity indices for the nine shipping routes. Columns (1), (3) and (5) show the results of the baseline regression. Columns (2), (4) and (6) are the regression results incorporating control variables. t -statistics using clustered standard errors are in brackets. *** and * indicate significance at the 1% and 10% levels, respectively.

TABLE A13 | OLS regressions of freight rates on conditional operating capacity (monthly data).

	(1)	(2)	(3)	(4)	(5)	(6)	(7)	(8)	(9)
	Fre ¹	Fre ²	Fre ³	Fre ⁴	Fre ⁵	Fre ⁶	Fre ⁷	Fre ⁸	Fre ⁹
Panel A: Fronthaul operating capacity index Cap _A									
Cap _{A,t-1}	1.176 (0.515)	-2.981 (-1.102)	-0.295 (-0.196)	-3.155 (-0.953)	-6.824* (-1.942)	-1.702 (-1.093)	-1.687 (-0.218)	0.913 (0.064)	7.756 (0.870)
Cap _{A,t-1} × Id _{t-1} ^H	-0.433 (-0.688)	-0.048 (-0.039)	-0.749 (-0.756)	-1.884 (-1.041)	-1.916** (-1.980)	-0.558 (-0.905)	-5.920* (-1.770)	-15.75*** (-2.615)	-3.623 (-0.501)
Cap _{A,t-1} × Id _{t-1} ^L	0.220 (0.345)	0.443 (0.454)	0.737 (1.128)	2.192 (1.129)	-0.306 (-0.355)	0.576 (1.358)	5.707* (1.933)	2.600 (0.336)	3.182 (0.623)
Fre _{t-1}	0.283** (2.311)	0.488*** (4.408)	0.349** (2.429)	0.166 (1.325)	0.312** (2.222)	0.306*** (2.937)	0.551*** (5.388)	0.458*** (6.305)	0.107 (1.375)
R ²	0.053	0.217	0.130	0.039	0.133	0.137	0.358	0.244	0.001
Panel B: Backhaul operating capacity index Cap _B									
Cap _{B,t-1}	-1.338 (-0.618)	-1.277 (-0.724)	1.857 (1.148)	1.571 (0.336)	-8.660** (-2.443)	-2.563 (-1.279)	-8.934 (-1.237)	5.720 (0.786)	-1.226 (-0.154)
Cap _{B,t-1} × Id _{t-1} ^H	-0.229 (-0.382)	-0.412 (-0.247)	-0.838 (-0.622)	-3.242 (-0.876)	-1.691** (-2.037)	-0.794 (-1.106)	-5.579 (-1.381)	-14.788** (-2.550)	-13.341 (-1.128)
Cap _{B,t-1} × Id _{t-1} ^L	0.421 (0.676)	0.951 (0.739)	0.414 (0.665)	2.394 (0.731)	-0.371 (-0.545)	0.800 (1.494)	3.302 (1.119)	5.708 (0.704)	9.422 (0.911)
Fre _{t-1}	0.270** (2.047)	0.470*** (4.279)	0.336** (2.274)	0.181 (1.358)	0.284** (2.147)	0.331*** (3.256)	0.550*** (5.859)	0.461*** (5.958)	0.108 (1.326)
R ²	0.054	0.212	0.131	0.029	0.155	0.149	0.345	0.258	0.009
Panel C: Total operating capacity index Cap _C									
Cap _{C,t-1}	-0.029 (-0.023)	-1.918 (-1.238)	0.398 (0.317)	-1.163 (-0.453)	-5.363*** (-2.618)	-1.603 (-1.316)	-5.460 (-0.992)	3.151 (0.645)	2.896 (0.469)
Cap _{C,t-1} × Id _{t-1} ^H	-0.163 (-0.531)	-0.119 (-0.161)	-0.482 (-0.854)	-1.227 (-0.960)	-0.870** (-1.972)	-0.341 (-1.021)	-3.052* (-1.718)	-8.176*** (-2.655)	-3.365 (-0.710)
Cap _{C,t-1} × Id _{t-1} ^L	0.173 (0.553)	0.339 (0.598)	0.264 (0.806)	1.301 (0.990)	-0.187 (-0.501)	0.363 (1.517)	2.160 (1.433)	1.971 (0.496)	3.006 (0.859)
Fre _{t-1}	0.278** (2.196)	0.472*** (4.446)	0.351** (2.329)	0.175 (1.378)	0.290** (2.196)	0.311*** (2.997)	0.544*** (5.816)	0.460*** (5.937)	0.107 (1.361)
R ²	0.051	0.217	0.128	0.033	0.159	0.149	0.354	0.253	0.001

Note: OLS regressions of freight rates on conditional operating capacity using the model: $Fre_t^i = \alpha_0 + \alpha_1 Cap_{j,t-1}^i + \alpha_2 Cap_{j,t-1}^i \times Id_{t-1}^H + \alpha_3 Cap_{j,t-1}^i \times Id_{t-1}^L + \alpha_4 Fre_{t-1}^i + \epsilon_t^i$. When idle capacity is higher than the 70th percentile, $Id_t^H = 1$. When idle capacity is lower than the 30th percentile, $Id_t^L = 1$. In all other cases, the indicator is 0. *t*-statistics, using Newey-West HAC standard errors, are in brackets. ***, ** and * indicate significance at the 1%, 5% and 10% levels, respectively.

TABLE A14 | Panel regressions of freight rates on conditional operating capacity (monthly data).

	Panel A: Fronthaul operating capacity index Cap_A		Panel B: Backhaul operating capacity index Cap_B		Panel C: Total operating capacity index Cap_C	
	(1)	(2)	(3)	(4)	(5)	(6)
$Cap_{j,t-1}$	-1.039*	-0.907	-1.064	-0.885	-0.954*	-0.842
	(-1.902)	(-1.550)	(-1.059)	(-0.883)	(-1.777)	(-1.479)
$Cap_{j,t-1} \times Id_{t-1}^H$	-0.713***	-0.732***	-1.023***	-1.033***	-0.435***	-0.442***
	(-4.405)	(-3.950)	(-5.076)	(-4.634)	(-4.896)	(-4.359)
$Cap_{j,t-1} \times Id_{t-1}^L$	0.661***	0.626***	0.762***	0.721***	0.379***	0.360***
	(6.337)	(7.776)	(6.112)	(5.920)	(7.730)	(8.425)
Fleet _t		-0.080		-0.075		-0.066
		(-1.095)		(-1.186)		(-1.023)
Export _t		-0.080		-0.078		-0.063
		(-0.171)		(-0.181)		(-0.137)
Fuel _t		0.054***		0.054***		0.054***
		(3.125)		(3.137)		(3.104)
Fre _{t-1}	0.314***	0.312***	0.317***	0.315***	0.315***	0.313***
	(4.208)	(4.225)	(4.248)	(4.263)	(4.234)	(4.249)
R^2	0.114	0.121	0.115	0.121	0.116	0.122

Note: Panel regressions of freight rates on conditional operating capacity using the model:

$Fre_t = \alpha_0 + \alpha_1 Cap_{j,t-1} + \alpha_2 Cap_{j,t-1} \times Id_{t-1}^H + \alpha_3 Cap_{j,t-1} \times Id_{t-1}^L + \alpha_4 Fre_{t-1} + \epsilon_t$. Columns (1), (3) and (5) show the results of the baseline regression. Columns (2), (4) and (6) are the regression results after adding control variables. When idle capacity is higher than the 70th percentile, $Id_t^H = 1$. When idle capacity is lower than the 30th percentile, $Id_t^L = 1$. In all other cases, the indicator is 0. *t*-statistics, using clustered standard errors, are in brackets. *** and * indicate significance at the 1% and 10% levels, respectively.